CHEMICAL REVIEWS

REVIEW

pubs.acs.org/CR

Linear and Nonlinear Optical Properties of Colloidal Photonic Crystals

Luis González-Urbina,[†] Kasper Baert,[†] Branko Kolaric,[*,‡] Javier Pérez-Moreno,[†] and Koen Clays[*,†]

[†]Department of Chemistry and INPAC—Institute of Nanoscale Physics and Chemistry, K. U. Leuven, Celestijnenlaan 200D, B-3001 Heverlee, Belgium

[‡]Laboratoire Interfaces et Fluides Complexes, Centre d'Innovation et de Recherche en Matériaux Polymères, Université de Mons, 20 Place du Parc, 7000 Mons, Belgium

CONTENTS

1. INTRODUCTION

Photonic crystals (PhCs) have set up a new trend in optical materials thanks to their potential to control the propagation of light in the linear and nonlinear regimes. These properties can find applications in telecommunications and electronics, as the current microelectronic technologies demand new building blocks to integrate photonics[1] in their hot and slow[2] semiconductor devices. Waveguides,[3] nanolasers,[4−6] superprisms,[7] and fiber-to-chip couplers[8] are being designed for this purpose. Aside from the manufacturing and technological limits, PhCs formed out of colloidal suspensions, or colloidal photonic crystals (CPhCs), offer a good scenario for the study of the physics behind the propagation of light in periodic media and an inexpensive testing ground for new discoveries.

These materials are not new, however. From ancient times human beings have been fascinated by the remarkable optical properties of colloidal crystals. The mystical opals and insects displaying iridescent colors (see Figure 1), incomprehensible for our ancestors, have turned into the models for the study of photonic crystals.

Regardless of this old fascination for opals and colorful exoskeletons, the modern nanophotonics is a relatively young branch of science, born almost 30 years ago when the fields of colloidal material science and modern optics merged. Nevertheless, many of the breakthroughs in the modern optical technology have resulted from a deeper understanding of the physics and the technology of colloidal materials.

Most of the electromagnetic phenomena are the consequence of the interaction of electromagnetic waves (light) with matter.[10] The structures of modern photonic and plasmonic[11,12] materials are designed by attempting to manipulate the properties of the electromagnetic waves. When the dimensions of the structures are in the order of the wavelength of the light, the interactions are better described using the laws of quantum mechanics. It is important to notice that the electromagnetic properties are scalable with the dimensions of the structures. This makes photonic materials easy to adapt to the requirements of the application regardless of the material used, which offers an advantage over semiconductors technology. This is possible because Maxwell's equations[13] do not have a characteristic length scale, which implies that the effect of the very short spatial periods of the electron densities interacting with the very short wavelengths of X-rays can be scaled up to much larger periodicities (as in colloidal crystals) corresponding to electromagnetic waves with much larger wavelengths (as the visible and infrared spectrum). Unfortunately, the periodicity of matter at such small dimensions is technologically very difficult to scale. The advances of nanoscience in the last few decades allow the achievement of periodic nanostructures, normally by means of very expensive and laborious techniques.[14] It is at this point that CPhCs provide an inexpensive approach used nowadays for experimental purposes but amenable to industrial processing.[15]

The concept of PhCs will be introduced in section 2 with an overview of the most common fabrication techniques. In section 3 the main feature of these structures, the photonic band gap (also named stop band), and its physical description will be explained,

Received: February 19, 2011
Published: December 23, 2011

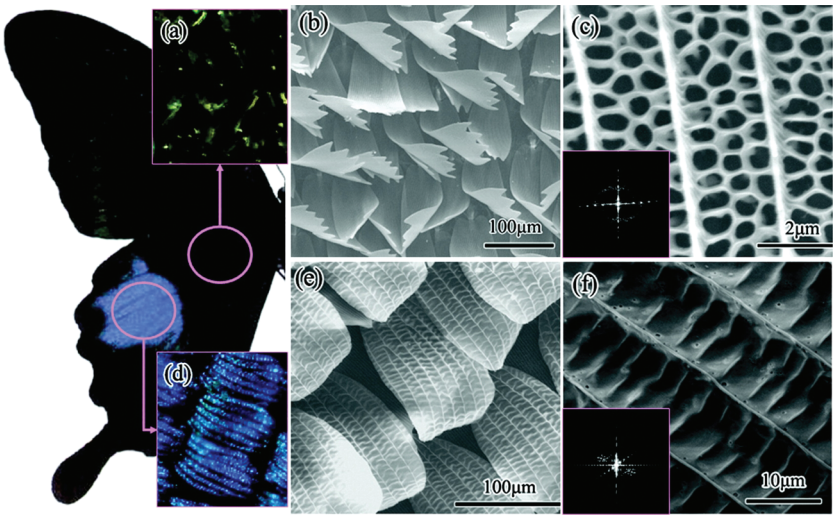

Figure 1. Morpho butterfly has become an emblem of natural photonics. In the figure, the images magnify parts of the photography of a blue butterfly wing, offering a (a) low-magnification optical microscopy image, (b) low-resolution field emission scanning electron microscope (FESEM), and (c) high-resolution FESEM image. Images (d)−(f) display the same sequence of microscopies for a black butterfly wing from the same species. The insets in (c) and (f) show the Fourier spectra from the images. The experiment[9] demonstrates that the different colors are caused by different nanostructures. Reprinted with permission from ref 9. Copyright 2009 American Chemical Society.

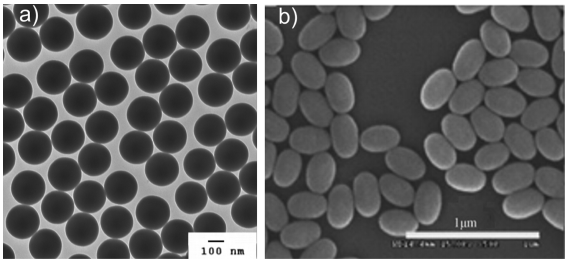

Figure 2. (a) Transmission electron microscopy images of spherical colloids (d = 223.8 nm) and (b) Fe_2O_3/SiO_2 core−shell ellipsoids with an aspect ratio of 1.5.[26] Reprinted with permission from ref 26. Copyright 2009 Wiley-VCH.

together with some tools for its modulation. Section 4 deals with the concept of band gap engineering and superlattices. Defects induced in the structure and the modes created due to the presence of the former defects leads to the concept of pass band. Fluorescence will be introduced in section 5, where we discuss how a photonic band gap, engineered to match the energy of the radiative transition, can inhibit the emission from a dye embedded in the structure. An account on how the emission suppression was afterward used to enhance energy transfer within the PhC is explained in section 6. The colloidal crystals also have been used to enhance nonlinear emission, either modifying the speed of the fundamental wave or allowing the phase matching of the generated beam, as will be analyzed in section 7, followed by the conclusions.

The primary goal of this review is to overview the optical properties of CPhCs for the chemistry audience from the perspective of physical chemistry, with a special emphasis on the radiation process and the energy conversion within the photonic structure, which is very often excluded from standard photochemistry books and review articles. Because the discussions of these topics are still open-ended, a chronological overview of the historical research and the progress made in this field during the last few years is given, together with clear explanations of the physics involved in these processes. Notice that we do not want to review everything or repeat previous efforts but will focus and refer the readers to other reviews when appropriate.

2. COLLOIDAL PHOTONIC CRYSTALS

2.1. Colloids and Materials

Conventionally, a colloid is a two-phase system, where one phase is dispersed in a second phase called the continuous medium.[16] A colloidal crystal is formed from solid monodisperse beads of particles, ranging from a few nanometers to the micrometer scale. The monodispersity of the nanoparticles is a key factor, because the periodicity of the structure will rely directly on the monotonic size of the beads, and therefore, unintentional different sizes cannot result in a periodic structure.

The most commonly used colloids in colloidal crystals are silica (SiO_2) spheres synthesized by the Stöber−Fink−Bohn method;[17] however they can be made out of other oxides, e.g., titania (TiO_2), also synthesized via hydrolysis of an alkoxide,[18] or ceria (CeO_2), although for the latter the hydrolysis offers poor control on the shape and it is normally produced with other methods.[19] Many polymers can be used in the synthesis of colloids, produced in many different polymerization routes.[20,21] Among the polymers, polystyrene (PS)[22] and poly(methyl methacrylate) (PMMA)[23] are the most employed. Colloids can also adapt different shapes[24−26] (see Figure 2). Interested readers can find details elsewhere.[27,28]

2.2. Deposition Techniques

The fabrication methods of CPhCs are low-cost, bottom-up techniques. The colloids intrinsic property of self-assembly is used in our favor to pack the particles in a three-dimensional (3D) periodic arrangement. A recent publication from López and co-workers[27] reviews self-assembly for ordered and disordered structures.

The most common of the methods available is vertical deposition,[29,30] driven by thermodynamic rules of minimum energy

conformation. The particles, suspended in the solvent wherein the substrate is vertically placed, are attracted to the meniscus of the liquid and, as the solvent evaporates, pile up in a close-packed fashion. The quality of the crystal formed depends on many closely related parameters,[31] for example, the size and material of the beads are dependent on the solvent employed, due to the compromise between evaporation rate and sedimentation. In fact, this compromise becomes problematic for large spheres. Other similar techniques like gravity sedimentation[32] and horizontal deposition[33] are based on the same principle.

Non-purely self-assembly techniques are electrostatic repulsion,[34,35] spin-coating template-assisted assembly,[36] physical confinement,[37,38] capillary forces-induced convective self-assembly,[39] and electric field-induced assembly.[40] Among forces driven methods, the most popular are spin-coating[41,42] and Langmuir−Blodgett.[43]

In spin-coating a very concentrated colloidal suspension is spun on a substrate rotating at high speed.[42] This technique has the advantage of the rapidness and that it allows the deposition of spheres that, for whatever physical reason, do not tend to self-assemble, and their deposition on surfaces is otherwise unsuitable for that purpose.[44] The major influence on the quality comes from the solvent chosen for the deposition, as a very volatile solvent will not allow the shear forces to impose the desired order whereas a low volatile solvent will lead to extremely long deposition times. The deposition of spheres in a polymer matrix has been reported[41,45] as being successful using a single-step process, giving rise to a noncompact packing. The resulting composite has no strong photonic effect as the contrast between the refractive index from the matrix and from the spheres (typically silica) is not high enough, but a selective removal of the spheres or of the matrix offers, respectively, a polymer inverse opal or a silica opal. The drawback of this technique falls on the quality of the crystal, which is composed of a circular distribution of rotated domains.

In the case of Langmuir−Blodgett, for which a very complete review by Bardosova can be found,[43] the absolute and precise control on each layer deposited is the best advantage. However, the tedium of this technique and the low packing efficiency between successive layers relegate this technique to research, where it is especially useful for controlled defect formations (see section 4).

2.3. Packing of Colloids

The preferential packing conformations for monodisperse spherical particles depend on the deposition technique employed for the crystal formation. Hexagonal close-packed (hcp) and face-centered cubic (fcc) are the most common lattices obtained. Using self-assembly techniques, the parameters chosen for the deposition dictate the final packing, but most of the time one deals with a mixture of both.[46−48] The mixtures of these two conformations is commonly denominated as random hexagonal close-packing (Rhcp). Here, the proportion of fcc seems to be higher for slow depositions, closer to thermodynamic equilibrium,[49,47,50] and for certain deposition methods.[51] Langmuir−Blodgett achieves a close hexagonal lattice for each layer, which normally would lead to hcp or fcc 3D structures, but the packing of layers proves to be inefficient. Although fcc packing is accepted, a good discussion can be found in the recent review from Bardosova.[43] External forces can also induce different packing orientations as was reported for the spin-coating technique.[42] The influence of the packing and materials on the photonic properties of the periodic nanostructures is discussed in the next section.

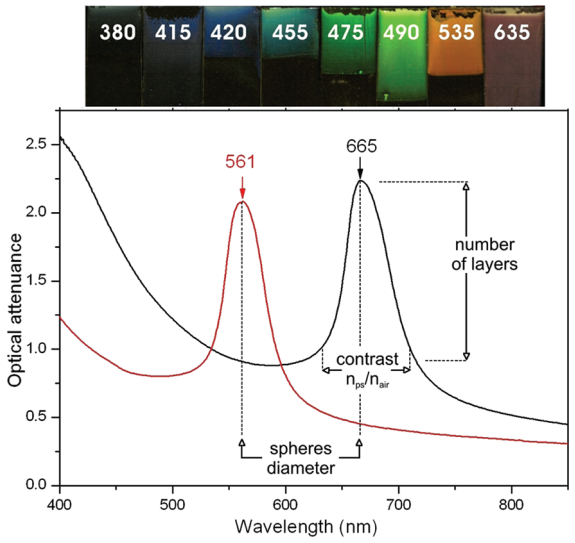

Figure 3. Typical optical attenuance spectra of colloidal photonic crystals from silica spheres of 258 nm (red) and 305 nm (black) diameter measured perpendicular to the substrate. On top of the spectra a picture shows 8 crystals, deposited by vertical deposition, arranged in increasing colloid size. The position of the diffraction peak is superimposed.

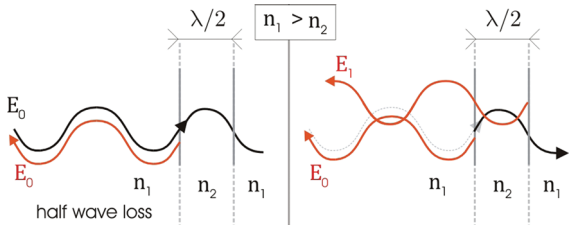

Figure 4. Example of destructive interference in the reflection of light in successive interfaces separated by $\lambda/2$. In the first interface, if $n_1 > n_2$, the beam is reflected with a phase shift of π (or half wave loss). At the second interface, after traveling $\lambda/2$ where the phase of the transmitted beam (E_0) has shifted π, it suffers a reflection with no loss. The reflected beam (E_1) covers the distance back ($\lambda/2$), with the corresponding phase shift (π), and it is transmitted at the first interface. The beams reflected in the first (E_0) and in the second (E_1) interfaces have a phase difference of $\pi + \pi + \pi = 3\pi \equiv \pi$, and the resulting interference is destructive.

3. PHOTONIC BAND GAP

Recalling that 3D colloidal crystals consist of a periodic array of macroscopic uniform colloidal particles distributed forming a repeating pattern, like atoms do in a crystalline solid, the comparison can be established with semiconductors.[52] The macrostructure can be considered as a crystal and the colloids are sometimes referred to as "dielectric atoms". The effect of this arrangement upon the propagation of electromagnetic waves can be described in terms of a band structure due to their ability to control photon propagation in the same way as semiconductors control the flow of electrons.[13] The periodic changes of refractive index within the colloidal crystal, i.e., crystal/voids, result in the appearance of a forbidden region of frequencies for photons. This region is called photonic band gap (PhBG), which is a

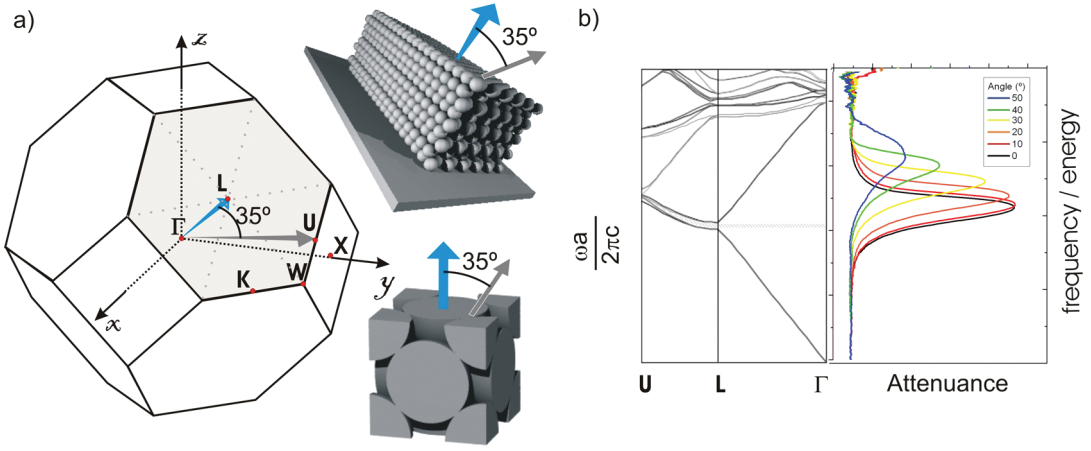

Figure 5. (a) Brillouin zone (left) for the fcc lattice (right): a truncated octahedron. The points Γ, L, U, X, W, and K correspond to the high symmetry points. The direction Γ−L (represented with a blue arrow coming from the center of the polyhedron to the center of the hexagonal face) is the direction normal to the (111) plane, the plane typically parallel to the substrate. The direction Γ−U (gray arrow) is a deviation of 35° from Γ−L and corresponds to the direction [411]. (b) represents the photonic band structure (left) for the two directions mentioned before. Note that there is no complete gap, but that there are some partial gaps (striped area). The band gaps in the dispersion curves can be assigned to the attenuance spectra for the different directions of propagation.

crucial parameter for molding the propagation of light. The typical optical attenuance spectrum of colloidal photonic crystals can be seen in Figure 3, where each band gap corresponds to a different colloidal size. The picture on top of the graph shows a series of photonic crystals deposited using vertical deposition. The reflected color wavelength corresponds to the position of the band gap in the visible spectrum.

3.1. 1D: Bragg Diffraction or Standing Wave

A simple way to get a physical picture of the band gap peak can be attained by picturing it as a diffraction peak formed by constructive and destructive interferences of light, which is caused by the multiple reflections and refractions from different crystal planes[53,54] (see Figure 4). To calculate the peak of the band gap, one must consider the amplitude of the refracted and reflected light but also the phase. For a long distance between the planes, the incident and reflected beams will not have any phase relationship and they will not interfere, but if the distance between planes is in the order of magnitude of the light wavelength and a multiple of a fraction of this, i.e., $\lambda/4$, $\lambda/2$, or $3/4\lambda$, the propagating waves will add, giving rise to constructive and destructive interferences. The nature of the interference will be dictated by the distance between planes, because the phase will depend on the distance covered, but also by the phase change at the interface when the second layer has a higher refractive index.

With this method it is easy to calculate roughly the position of the peaks in terms of the thickness and the refractive indexes:

$$\lambda_{peak} = 2d\sqrt{n_{eff}^2 - \sin^2 \alpha} \quad (1)$$

where λ is the wavelength of the incident light, d is the distance between planes, α is the angle of incidence, and n_{eff} is the effective refractive index[55] of the crystal, calculated as follows:

$$n_{eff} = \sqrt{f \cdot n_{ps}^2 + (1-f) n_{air}^2} \quad (2)$$

where f is the filling factor, n_{ps} is the refractive index of the particles, and n_{air} is the refractive index of the voids, normally filled with air. For a close-packed structure the filling factor is $f = 0.74$. As previously discussed, most deposition techniques lead to fcc or hcp structures. In both cases the crystallographic plane (111) is formed parallel to the substrate.[56] Therefore, the observed band gap at normal incidence is the Bragg diffraction peak of the (111) plane of the colloidal crystal, which can be calculated by eq 3

$$\lambda_{peak} = 2Dn_{eff}(0.816) \quad (3)$$

where D is the diameter of the spheres and the constant 0.816 is taken from trigonometric calculations to adjust the distance between planes for a close-packing of spheres. For colloidal particles with sizes from 200 to 400 nm and typical refractive indexes around 1.4, the peak falls in the visible region of the electromagnetic spectrum.

This method allows one also to estimate the amplitude of the reflected and transmitted waves. The Fresnel equations,[57] for the case of normal incidence, state

$$R = \left(\frac{n_1 - n_2}{n_1 + n_2}\right)^2 \quad (4)$$

where R is the reflected fraction. The quadratic character of this equation makes R always positive and bigger as the difference between n_1 and n_2, i.e., the refractive index contrast, increases. This equation relates the strength of the band gap to the materials used, as a higher refractive index contrast will reflect a more intense beam (E_1). Materials such as TiO_2 ($n \approx 2.5$), ZnS ($n \approx 2.36$), and some polymers are good candidates.

3.2. 3D: Dispersion Curves in the Brillouin Zone

To go beyond the 1-dimensional picture, solid-state physics makes use of the Brillouin zone[58] (see Figure 5a), a characteristic feature from crystallography to characterize the solutions for the wave (wave function[59]) crossing the PhC. The Brillouin zone is to the reciprocal space what the unit cell is to the real space. The reciprocal space is directly related to how the photon sees the material, and it defines the areas and boundaries that affect the movement of an electromagnetic wave. The Brillouin zone concentrates in a single diagram (see Figure 5b) this reciprocal space for a periodical structure, e.g., for a colloidal crystal, and like

dx.doi.org/10.1021/cr200063f |Chem. Rev. 2012, 112, 2268–2285

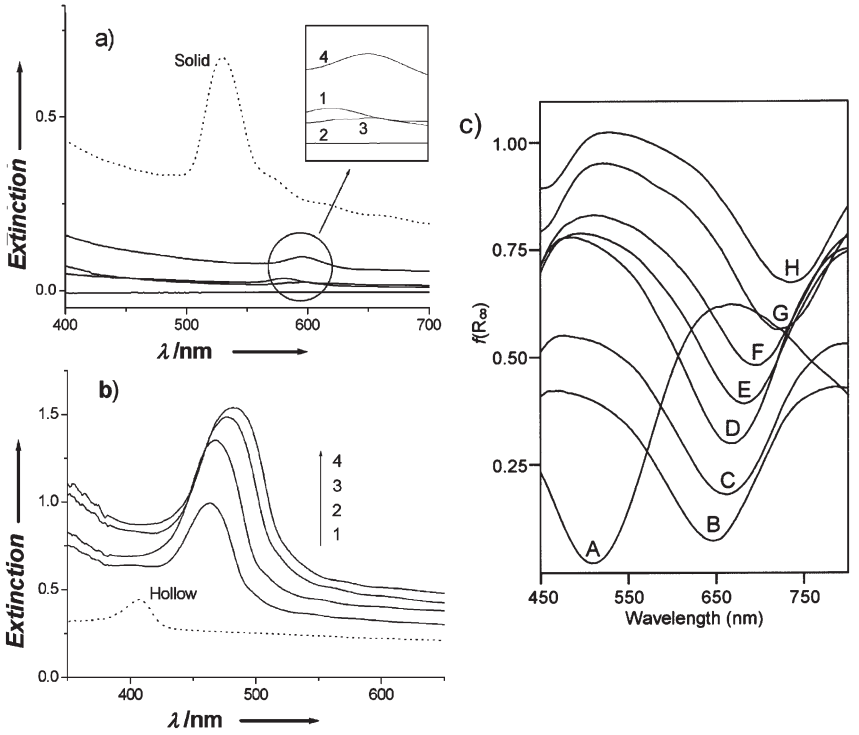

Figure 6. Attenuance spectra, in dot lines, of CPhCs made up of (a) silica spheres and (b) air-core/dense-silica-shell hollow spheres. In solid lines the effect upon infiltration with different liquids is depicted: (1) ethanol; (2) dimethylformamide; (3) toluene; and (4) 1,2-dibromoethane. Modified from ref 72. Copyright 2008 American Chemical Society. (c) PhBGs measured in reflectance of ZrO_2 (285 nm) with voids filled with fluids of different refractive indices: (A) air, (B) methanol, (C) ethanol, (D) 2-propanol, (E) tetrahydrofuran, (F) dimethylformamide, (G) toluene, and (H) 1,2-dibromoethane.[71] Reprinted with permission from ref 71. Copyright 2002 American Chemical Society.

in crystallography, by defining the critical points of the lattice it is possible to plot the frequencies allowed in each direction and the band structure of the crystal.[52]

The Brillouin zone represented in Figure 5a corresponds to a fcc lattice, and so does the dispersion diagram in Figure 5b. The band gap is marked with a striped area in the graph. Only the dispersion curves for the directions Γ−L and Γ−U are represented in order to concentrate the explanations on the commonly obtained result, i.e., the fcc structure with the plane (111) parallel to the substrate. Direction Γ−U would correspond to an inclination of 35° from the normal. Notice, in the dispersion curve, that the band gap shifts to higher energies as the angle increases. This corresponds to the attenuance measurement from a real CPhC, plotted in Figure 5b. The dispersion curve is therefore dependent on the Brillouin zone, which itself depends on the packing of the colloids.

The position of the band gap would vary for nonclose-packed structures and for inverse opals. The result can easily be deduced from eqs 1 and 2. In the first case, f will be smaller, and this will reduce the n_{eff} making also smaller the λ_{peak}, and the PhBG would shift to higher energies. For the inverse opal, it is more interesting to see the evolution of the PhBG position along the whole fabrication process. First, when the structure is infiltrated with the high refractive index material, the n_{eff} will clearly increase and so will do λ_{peak}. Once the colloidal material is removed, the position of the resulting PhBG will depend on the refractive index of the new material but in any case, it will move back to higher energies. A clear example can be found in the paper from King et al.[60]

As the contrast in the refractive index increases, a broadening of the gaps is induced in the dispersion curves along the Γ−L and Γ−U directions. For high enough contrast, an opening of a full PhBG at higher frequencies can be observed. In the work from Marichy et al.,[61] simulations of the band structures for the infiltration process of a silica opal with titania, and after the subsequent removal of the silica, can be found.

Summarizing, the main characteristics of the PhBG are the position, the amplitude, and the width. The position of the PhBG depends on the size of the spheres (for a given material), the amplitude or attenuance strength will be defined by the number of layers forming the sample, and the width will be given by the refractive index contrast, as it can be deduced from the dispersion curve (in Figure 5). These parameters can be seen depicted in Figure 3.

A very popular tool to model the PhBG is the finite-difference time-domain method (FDTD).[62,63] This method solves Maxwell's differential equations using an iterative approach. The components for an arbitrary electric field (E-field) vector are set for certain time and position, and the components for the magnetic field (H-field), dependent on the change of E-field through the curl, are calculated. The results from the latter are used to recalculate the first ones, and those for the second ones, until the solution becomes stable. The method is applicable to 3D using Yee cell,[64] which divides the electric and magnetic components for the six faces of a cube.

3.3. Full Photonic Band Gap and Inverse Opals

Strictly speaking, the PhBG obtained typically in CPhC is a pseudogap, because it does not forbid the propagation of one

wavelength in all the directions; even more, the affected wavelength varies with the incidence angle. A full PhBG blocks the propagation of certain energy photons in all the directions. In a hcp lattice with low refraction index contrast, characteristic of CPhCs, the formation of a full PhBG is highly unlikely. In contrast, a diamond lattice, even when using a material with a low refractive index, allows the formation of an almost complete band gap.[65] A diamond-lattice structure can be realized by means of lithography, two-photon polymerization,[66] or microrobotic techniques.[67] Hence, the engineering of a full band gap CPhC has not yet been realized experimentally in the visible regime.[68] Nevertheless, due to the huge potential applications, the design of a complete band gap in the optical range is still one of the final goals of modern nanophotonics. A recent approach achieves an almost complete band gap from low refractive index colloids, like silica or polystyrene particles, by depositing the colloidal crystal on a curved substrate due to the numerous refractions and reflections on the bended surface.[69,70]

Additionally, colloidal crystals are useful as templates for the fabrication of inverse opals, which can improve the photonic band gap properties. This is based on the infiltration of a material with a high refractive index in the voids of the opal, eventually followed by the removal of the beads, in order to increase the modulation of the refractive index[71] and to lower the filling factor[72] (see eq 2). The results are summarized in Figure 6.

Inverse opals might, therefore, lead the way to obtain a full PhBG, by virtue of using CPhCs as the basis for their fabrication. Currently, a full PhBG for high-energy regimes from a silicon inverse opal has been reported.[73]

4. DEFECT MODES AND BAND GAP ENGINEERING IN CPHCS

The analogy of photonic crystal with semiconductors goes beyond the formation of a forbidden energy gap for the carriers. In a similar way that defect modes can be created in semiconductors by doping, it is possible to create regions inside the PhBG where only a range of wavelengths is allowed to cross, by the introduction of defects. The type of defects can be classified using crystallographic terminology,[74] because CPhCs form lattices. Natural defects can always be found in CPhCs, including vacancy defects, defect lines, misaligned domains, and cracks. Nevertheless, it has been proven that, overall, the artificial colloidal opals have good quality and the properties of a single crystal.[75]

Still, defects can be introduced intentionally. As a result, the presence of an interruption in the periodicity creates a defect mode and causes a dip in the band gap. This depression is called a pass band, for its similarity with the signal-processing filters.[76] The position of the pass band is, again, dependent on the nature of the defect, i.e., on the refractive index, on the size of the defect itself, and, as the band gap, on the angle of incidence.[77]

4.1. Defect Formation Techniques

Many different techniques have been proposed to break the periodicity of the colloidal lattice in a controllable way. A point defect in a CPhC becomes a microcavity of a high-quality factor,[78] due to the strong localization of light. This feature is interesting for light-emitting diodes and low-threshold lasers, and it will be introduced in section 5.3. Point defects in a CPhC have been created by lithography[79] with total control on the position and size, taking advantage of the intrinsic property of the colloids to self-assembly.

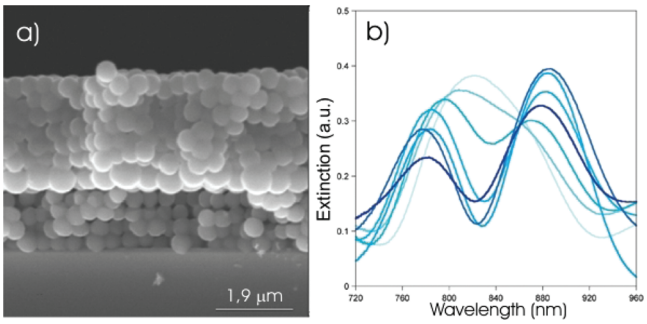

Figure 7. (a) Scanning electron microscopy (SEM) side view of a $(390\ nm)_4/(590\ nm)_1/(390\ nm)_6$ stack and (b) experimental near-infrared (NIR) transmission spectra of colloidal crystals with a defect layer located at different relative positions inside the heterostructure.[92] Reprinted with permission from ref 92. Copyright 2009 American Chemical Society.

A defect line in a PhC is in effect a waveguide. CPhCs have been used as a template to fabricate inverse opals where a defect line has been introduced[80] by multiphoton polymerization previous to the normal steps of infiltration and beads removal.

Planar defects can be introduced in many different forms, and the nature of the defect layer is variable, as it is the way for its deposition: Langmuir–Blodgett,[81,82] chemical vapor deposition,[83] or spin-coating.[84] To deposit a layer from a polymer or from small particles, spin-coating is a suitable technique,[85,86] whereas for spheres deposition, Langmuir–Blodgett offers the best control over the number of layers.[87–90]

In purely CPhCs the defect is a layer made up of different spheres to those where they are sandwiched in between. The spheres must be either from a different material[91] or of a different size. At the same time, the pass band created will depend on the type of planar defect introduced.

4.2. Donor–acceptor Modes through Different Colloid Sizes

CPhCs with planar defects made up of spheres of a different size were achieved by Wostyn et al.[81] by combining vertical deposition with Langmuir–Blodgett. In all the cases, the defect they introduced consisted of a monolayer of spheres bigger than those of the surrounding opal. When they kept the size of the latter constant, the position of the pass band moved across the band gap, because the cavity, i.e., the diameter of the spheres in the defect, increased. They compared this effect with the donor–acceptor modes in semiconductors and determined that an increase in the size of the defect will create a donor mode, which is closer to the short-wavelength edge of the PhBG, which would be the equivalent of a conduction band in semiconductors. The counter-effect, an acceptor mode, was later reported in a publication by Massé et al.,[92] where the position of the defect layer within the whole superlattice was also studied. The best crystal conformation was found for a defect layer made out of spheres that were smaller than those making up the host and located at the center of the superlattice, because a monolayer of big particles distorts the upper layers. Part of this work is displayed in Figure 7.

4.3. Role of Refractive Index

A good example of this possibility can be found in the paper by Massé et al.[92] where the experimental results are supported by theoretical calculations based on FDTD. To this aim, the researchers combined in their paper three techniques for the deposition of multilayers (vertical deposition and Langmuir–Blodgett) and

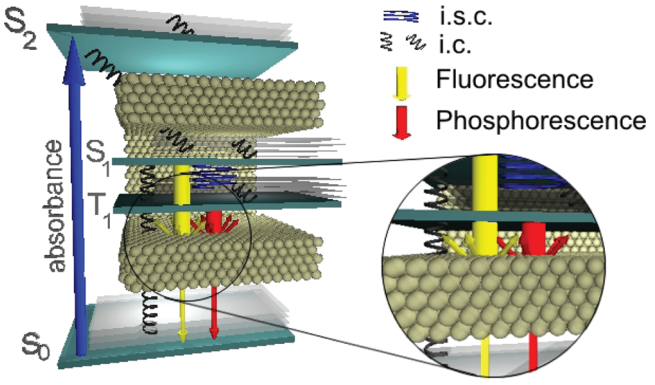

Figure 8. Representation of the Jablonski diagram under the influence of a CPhC, showing the ground state (S_0) and the first (S_1) and second (S_2) singlet excited states. The first triplet state is also shown (T_1). The absorption of a photon is depicted with an upward arrow. Spiral downward arrows indicate internal conversion (i.c.) and intersystem crossing (i.s.c.) (nonradiative transitions). Both fluorescence and phosphorescence are shown in full downward arrows. In the inset it is highlighted how the colloidal photonic crystal interferes with the radiative emission but has no effect on the nonradiative processes.

monolayers (Langmuir−Blodgett and horizontal deposition[93]), conditioned by the nature of the spheres. The advantage of using spheres of a different material but with the same size for the defect layer is that the disorder induced in the other case is minimized.

In their approach also two cases are possible. If the refractive index of the defect layer is bigger than that of the host layers, a donor mode is observed, and the pass band is blue-shifted from the center of the band gap. In the case of a defect layer made up of a material with a refractive index lower than that of the host layers, an acceptor mode is observed, and the pass band appears on the red side of the band gap.

Other superlattices can be designed, such as the ones used[94] to narrow the luminescence from an emitter embedded in the CPhC. The effect of the emission suppression in an opal is developed in the following section.

5. FLUORESCENCE IN CPHCS

It is well-known that fluorescence is the process of radiative (light-emitting) deactivation of a molecule that has been previously excited. The excitation might occur in different ways. When the electron is promoted to the excited state by a chemical reaction, the process is called chemiluminescence and if by an electric field, electroluminescence, but it can also be mechanically, with sound or with heat. However, all these different kinds of luminescence share the same physics of radiative deactivation. In 1852[95] Stokes named the phenomenon of radiative deactivation as fluorescence "to denote the general appearance of a solution of sulfate of quinine and similar media". The name is derived from the mineral fluorite (calcium fluoride), which fluoresces due to the presence of divalent europium. In turn the name fluorite derives from the Latin root "fluo", to flow. This makes the word fluorescence to derivate, indirectly, from the word "flow". The flow of energy in a fluorescence molecule or atom is normally schematically plotted in the Jablonski diagram.[96] In Figure 8 the Jablonsky diagram has been adapted to include the interaction of fluorescence with the CPhC.

After the system absorbs the energy, it will be excited to a vibrational level ($\nu = 0, 1, ...$) in the first excited state (S_1) or in a higher one (S_2, ..., S_n). Internal conversion will bring the system to the fundamental vibrational level ($\nu = 0$) in the first exited state by a rapid deactivation. The system then has three paths to relax. First, it can deactivate via a nonradiative way. Second, it might fall to a triplet state via intersystem crossing (without photon emission) and then emit a photon in a process called phosphorescence. And last, it can emit a photon decaying from the S_1 to the S_0 state. The last process is the fluorescence, a spin-allowed transition with transition rates around 10^8 s^{-1}. Because of the loss of energy (from S_n to S_1 and from the vibrational levels), the emitted light has a lower energy, and therefore longer wavelength, than the absorbed radiation. All these processes of relaxation are a consequence of the interaction of the system with the characteristic electromagnetic modes of the environment.

Fluorescence is, therefore, the emission of a electromagnetic wave, which can be influenced by the PhBG as was predicted by Yablonovitch already 30 years ago.[97] John and Wang[98,99] presented a theoretical investigation on the formation of photon-atom bound states for an atom in a PhC. When this phenomenon occurs, a reduction in the emission intensity in the energy range of the band gap is observed. This reduction is a consequence of the change in the lifetime (τ) of the excited states, because any emission process is dependent on the coupling with the environment. Also the decay occurs via optically driven electron−phonon interactions or via two-photon spontaneous emission depending on the nature of the material where the dye is located. A splitting of the excited energy level is predicted when the atom transition frequency lies near the band edge.[100] An overview of the discoveries made in this topic is given next.

5.1. Fluorescence Suppression

Fluorescence suppression and the dependence with the angle was reported by several groups and for different configurations. Bogomolov et al.[101] fabricated artificial opals by precipitating SiO_2 colloids and examined their optical properties. They observed how the stop band shifts upon deviating from normal incidence in transmission and upon changing the observation angle for the fluorescence of rhodamine 6G. Similar results for dye-doped polystyrene PhCs were reported by Yamasaki and Tsutsui[102] and for CdS infilled opals by Blanco et al.[103]

The presence on the nanostructure's surface of fluorophores, which are not affected by the PhC, makes it difficult to evaluate the full effect of the PhBG on the fluorescence. In fact, fluorescence from embedded emitters does not only originate from the outermost layers but from the entire crystal. Observations[104] that the PhBG seems shallower and less wide in a fluorescence experiment compared to transmission experiments were explained through a mechanism of diffuse light scattering as the crystals scatter more strongly near a band gap. This was later confirmed when similar effects were seen for a dye covalently bound to the interior portion of the crystal,[105] as shown in Figure 9. A photonic structure with the PhBG at the emission frequency of the fluorophore but where the emitter was selectively attached to only few layers in the center of the whole stack (see inset Figure 9b) was engineered. A second stack with the PhBG far from the emission wavelength was used as reference. It was shown that the PhBG created in a silica CPhC is incomplete and that it cannot suppress the omnidirectional emission of the sources.

5.2. Density of States

To understand the mechanisms taking place for the suppression, a deeper study of the radiation process is needed, and the

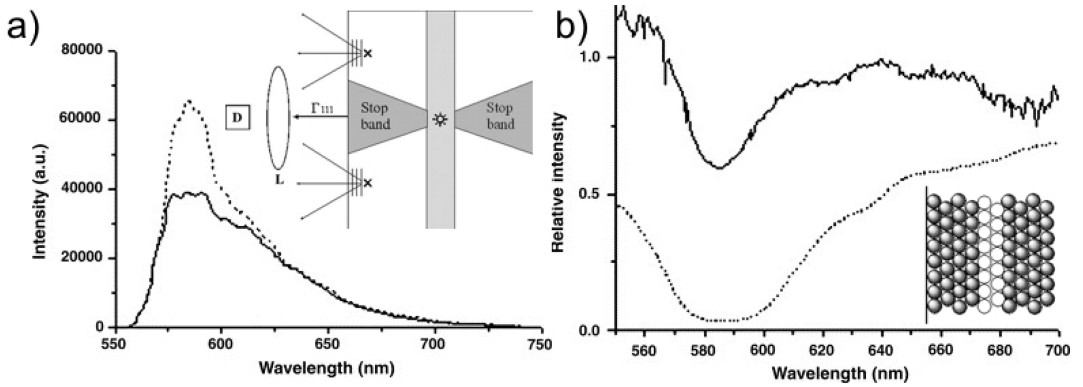

Figure 9. (a) Emission spectra (solid line) of a dye in a sandwich-like sample (see inset to b) and in a reference sample (dashed line). (b) Relative emission (solid line) and transmission (dotted line) spectra of the sandwich-like sample. A schematic illustration of the omnidirectional propagation and back-scattering of emission from photon point sources embedded in a sandwich-like sample is given as inset to a. L, lens; D, diode.[105] Reprinted with permission from ref 105. Copyright 2006 Elsevier.

study of fluorescence deals with the influence of parameters inherent to luminescence, such as the bleaching of the emitter or the environmental influence on the dye. This was a relevant issue on the results from the first report on modified emission originating from a 3D PhC,[106] where they reported inhibition of the radiative decay of a fluorophore, Kiton Red S, in an ordered aqueous suspensions of polystyrene microspheres. The effect, measured by means of pump−probe techniques, was attributed to the extinction due to Bragg reflection. However, in subsequent experiments by Tong et al.[107] using a time-correlated single-photon-counting technique, it was shown that a large fraction of the effect described before[106] could be ascribed to a local photon-field interaction with the emitter (colloid−dye interactions) combined with the high dye concentration used, in particular when taking into account the considerable overlap between the absorption and emission spectra of the fluorophore leading to reabsorption and reemission.

Experimental modifications were needed to prove the photonic effect on the emission decay kinetics. Doing this, Petrov et al.[108] reported nonexponential decay kinetics from a dye (1,8-naphthoylene-1′,2′-benzimidazole) solution in PMMA in the voids of a SiO_2 opal and supported this result by demonstrating spectral modification compared to a film of the polymer with the same infiltrated dye. The nonexponential decays comprised both inhibited and accelerated components, whereas the average decay time remained fairly unchanged. This was attributed to a redistribution of the photon density of states (DOS) available. This claim was challenged by Megens et al.[109] They held that the difference reported between accelerated and inhibited decay times was larger than could be accounted for by theory, and from their experiments on crystals built from colloids with a layer of embedded chromophore, they saw no such nonexponential behavior. This contradiction led to the conclusion[110] that the difference of location of the dye, uniformly distributed in the high-index material versus a narrow layer in the high-index medium, changes the local density of photon states experienced by the fluorophores. The implication was that the dye molecules in the thin shell experience a much more uniform photon DOS than those distributed throughout the high-index region. Subsequently Megens et al. reported[111] fluorescence investigations from dye molecules bound on a shell inside the colloids where they observed the spectral modification as expected. The excited-state lifetimes of the dye remained largely unchanged whether the colloids formed a PhC structure or not, but they did observe a change in lifetime on changing the collection wavelength, decreasing linearly until a certain wavelength, after which it rapidly increases. This wavelength dependence was interpreted as originating in the increased density of optical modes per unit volume available at shorter wavelengths, because the density of optical modes depends inversely on the wavelength.[112]

A theory based on DOS turned out to be needed to explain the observations on one of the first accounts of the use of inverse titania opals to influence fluorescence from embedded emitters,[113] where a double stop band at higher collection angles of the fluorescence was reported. These spectral features were confirmed by reflection spectroscopy and led them to conclude that simple Bragg diffraction does not suffice to explain light transport through PhCs. Using organic dyes for their large inhomogeneous and small homogeneous linewidths absorbed in the voids of an inverse TiO_2 opal to probe the DOS over a large frequency range, Koenderink et al.[114,115] observed large inhibition of the spontaneous emission by the PhC due to its modification of the DOS. They concluded that it is necessary to take the local DOS (LDOS) into account, rather than to average the DOS over the unit cell, as was often done. Locally the DOS varies much more over a given frequency range compared to the average over the unit cell, and it is this LDOS that is probed by the dyes in the inverse opal instead of the unit cell averaged one. They predicted that time-resolved decay measurements performed on dyes with high quantum efficiency would show as a composite of decay curves rather than as a single exponential, as was confirmed experimentally later.[116,117] Both inhibited and accelerated decay rates were observed from quantum dot emitters in an inverse titania opal,[118] offering control on the radiative decay through the engineering of a PhC over both a much wider frequency range and a much larger volume than typically afforded by a cavity. Also the enhancement of the emission at the blue edge of the crystals,[119] both for inverse and direct opals, cannot be explained through a standing wave picture but can be explained through a diffuse light model, the framework for which was described earlier.[120] The influence of a higher-order stop band of an opal on fluorescence emission was reported in the same article.[119]

From a microscopy experiment, backed by theoretical calculations, Barth et al.[121] found that, for relatively low index contrast crystals, e.g., polystyrene−air, there still are significant changes to

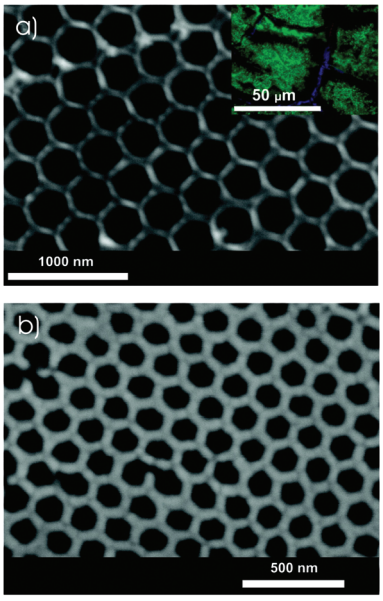

Figure 10. SEM images of the inverse silica opals made from a polystyrene opal template. The green iridescence from the sample can be seen in the photomicrograph inserted in (a).[123] Reprinted with permission from ref 123. Copyright 2007 American Chemical Society.

the emitted radiation and that redistribution of the optical DOS is also an important mechanism for emission modification. Notably they observed nonexponential decay curves from their organic dyes but did not attribute these to PhC effects. This redistribution of the optical DOS was subsequently investigated by Li et al.[122] in magnesium silicate inverse opals using a rare earth ion, viz. Eu^{3+}. They paid special attention to the angle dependence of the emission. A lifetime enhancement of rare-earth ions, Tb^{3+} in this case, in inverse opal PhCs (see Figure 10) was reported by Aloshyna et al.[123]

In another letter, Barth et al.[124] reported the first observation of single quantum dots inside PhCs and how, using a defocusing technique, they observed the extra anisotropy added by the stop band of the PhC even for a single emitter. Another experiment using quantum dots was performed by Nikolaev et al.[116] investigating the nonexponential decay curves observed in inverse 3D PhCs, explaining these by a continuous distribution of decay rates. This distribution was linked to the distribution of the emitters inside the unit cell of the crystal, suggesting that it is not necessary to have a complete PhBG to achieve spontaneous emission suppression or strong enhancement, but that a careful position control of the emitters inside the unit cell could do this.[125] The validity of this approach was confirmed by Vallée et al.[117] for silica opals, using organic dyes. Further insight in the directionality of emission was provided by Brzezinski et al.[126] by showing solid-angle resolved emission patterns of >76% of the available angles on one side of the fluorescent PhC. The PhC here was an inverse opal built up of ruthenium trisbipyridine $[Ru(bpy)_3]^{2+}(PF_6^-)_2$. Vion et al.[127] also performed angle-resolved experiments, on silica−air opals, measuring the fluorescence decay curves at different angles.

5.3. Lasing

Another important phenomenon in synthetic opals, namely, lasing, was first reported by Yoshino et al.[128] Using polystyrene inverse opals infiltrated with rhodamine 6G in methanol, not only did they observe inhibited spontaneous emission but they also induced spectral narrowing of the emission at high input powers. In a subsequent letter[129] the effect is attributed to optical feedback in the opal matrix, and they explain how they observed spectral narrowing and sharp emission lines on infiltration of the emitters in voids of the silica opals with a reflection peak matching the emission spectrum of the emitter. The periodic structures decrease the lasing threshold compared with disordered structures. On introducing an index-matching liquid, these features disappeared at constant input power, demonstrating the role of the photonic structure on the observed phenomenon. Stimulated emission attributed to resonance effect in photonic crystals has also been reported in sandwich-like hetero-opals, i.e., two stacks of CPhCs of different sphere sizes together, impregnated with luminescent CdTe nanocrystals.[130] As the constituent stacks of this hetero-opal have stop bands at different wavelengths, anisotropic reflection and emission spectra were observed. Specifically, the emission depends strongly on from which side of the interface light was collected and on the excitation power. The latter, together with the appearance of a minimum of transmission between the two respective stop bands, suggests a contribution of stimulated emission due to an interface resonance. The photonic band gap has the potential to modify the DOS and in this way alter the emission from the material embedded in the sample, which has been used to design low threshold lasers and single photon sources.[4−6,131]

5.4. Electroluminescence in CPhCs

Electroluminescence in 3D PhCs was reported by Kaplan et al.[132] They used chemical bath infiltration to fabricate SiO_2−Zn_2SiO_4:Mn and SiO_2−GaN−ZnS:Mn composite opals. The electroluminescence signal, excited by an AC electric field, shows anisotropy in concordance with the angular dependence of the PhBG measured in reflection. Further work on photoluminescence of complex inverse opals was performed by King et al.,[133] who used the atomic layer deposition technique to control both the refractive index and the luminescent properties. The effective refractive index could be tuned by changing the thickness of the infilled TiO_2 layer and the luminescent properties by the doping of the ZnS layer used. Another way of tuning the effective refractive index was reported by Paquet et al.,[134] who used capillary forces to insert PbS quantum dots in the voids of a PhC built up of PMMA colloids.

The interaction between different fluorophores also raised interest. Energy transfer in CPhCs is the topic treated in the next section.

6. FLUORESCENCE RESONANCE ENERGY TRANSFER IN CPHCS

One interesting phenomenon related to fluorescence is Förster energy transfer. The Förster effect, or fluorescence resonance energy transfer (FRET),[96,135,136] is well-known in biology because it takes part in a large variety of phenomena in nature, e.g., photosynthesis,[137] and was originally used to measure the distance between molecules. In a Förster process the donor, a fluorescent molecule in an excited state, transfers its energy to the acceptor. This can only happen if the donor emission wavelength corresponds to the acceptor absorption wavelength, in other words, if there is an overlap between the absorption spectrum of the acceptor and the emission spectrum of the donor, as is depicted in Figure 11.

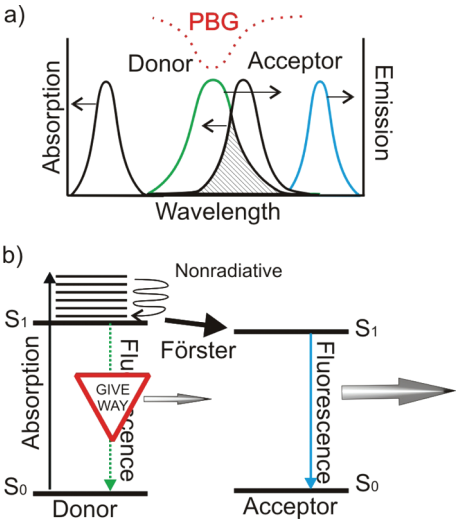

Figure 11. Förster energy transfer in the presence of a PhBG. (a) The overlap of the donor emission band and the acceptor absorption band is a requirement for this transfer to happen. The PhBG suppresses the emission from the donor. (b) Example of the mechanism for an energy transfer process between singlets. The suppression of the emission from the donor by the PhBG enhances the energy transfer, and in turn the emission from the acceptor increases.

Even though FRET is called fluorescence resonance energy transfer, it is purely a nonradiative process, which competes with fluorescence and other nonradiative processes. FRET is the result of a dipole−dipole interaction and, hence, is very sensitive to the distance between the molecules taking part in this process. Accordingly, the efficiency of this process is inversely proportional to the sixth power of the intermolecular separation. The normal distance[138] for FRET to happen lies between 10 and 100 Å. The transfer is very fast, $<10^{-9}$ s, and normally between singlet states, but it can also involve triplet states:

$$^1D^* + {}^1A \rightarrow {}^1D + {}^1A^*$$

$$^1D^* + {}^1A \rightarrow {}^1D + {}^3A^*$$

Subsequently the energy might be radiatively emitted from the acceptor molecule.

The study of FRET started before the publication by Förster in 1948,[139] but it was he who developed the first theories. Later theoretical works predicted that the resonance dipole−dipole interactions could be enhanced in confined geometries.[99,140,141] The initial experiments from Folan et al.[142] in 1985 on the energy transfer between molecules in micrometer-sized droplets, where Mie scattering enhanced energy transfer rates (k_{ET}), were studied later by Andrews,[143] who knew about the possibility to extend this theory to Förster energy transfer.[144,145] The studies led to the publication of two experimental works about FRET in an optical microcavity.[146,147] In these publications, the distance between donor and acceptor was controlled by using layers of a transparent material and by confining the system with silver mirrors. In both cases, the linear dependence of the energy transfer on the donor emission rates (k_d) was observed, demonstrating the importance of the distance between the donor and the acceptor. The influence of the confinement was also observed and attributed to the modification of the density of photonic modes. Fermi's golden rule was proposed to link the transfer rate

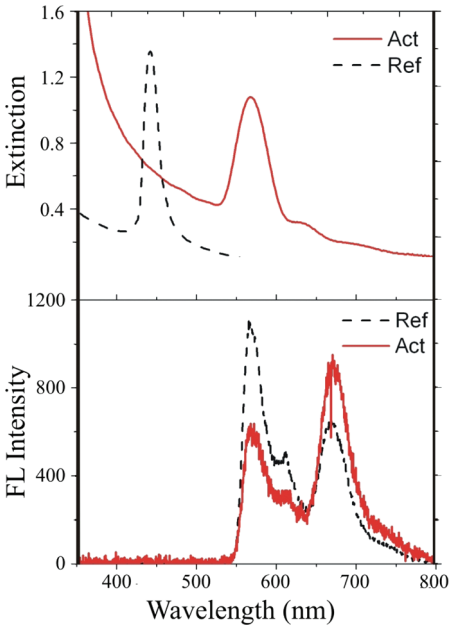

Figure 12. On the top, extinction spectra for the active and reference PhCs. On the bottom, fluorescence spectra of Cy3 and Cy5 dyes embedded in a photonic crystal with the band gap suppressing the emission from the donor (solid red line) and without suppression (dashed line), measured using a confocal microscope.[150] Modified and reprinted with permission from ref 150. Copyright 2007 American Chemical Society.

and the cavity photonic modes.

$$k_{ET} \propto k_d = \left(\frac{\pi}{2\hbar^2}\right)|\mathbf{M}_{ij}|^2\rho(\omega) \quad (5)$$

where $\rho(\omega)$ is the density of final states and $|\mathbf{M}_{ij}|$ is the matrix element for the donor transition. The suggestion of controlling the transfer by modifying the optical environment was supported with analysis of emission decay profiles also for microspherical cavities,[148] where it was stated that the enhancement could not be explained simply by radiative energy transfer.

Given the Fermi golden rule, it is obvious that a structured environment like a 3D PhC can be used for controlling the DOS. The emitter−environment coupling allows us to control the emission of light by modifying the surroundings of the dye without the expensive and time-consuming protocols of synthetic chemistry.

The first account on enhancement of energy transfer using the photonic properties of colloids was reported by Shibata et al.[149] They used a concentrated suspension of silica particles in water where two molecules, rhodamine B and rhodamine 110, were dissolved. The efficiency of energy transfer was enhanced in the presence of colloidal crystals when the Bragg peak wavelength matched the emission band of the donor, rhodamine 110. However, because of the low concentration of the dyes on the suspension, which entailed too large distances for FRET, and because of the lack of correlation with the crystal size, the authors concluded that the main transfer mechanism should be radiative transfer, i.e., emission and reabsorption, enhanced due to the scattering and to photon trapping in the colloidal suspension.

Förster energy transfer in CPhCs was successfully brought to practice recently.[150] In this experiment the distance between

FRET pairs was controlled using oligonucleotides, a double-strand backbone that was formed from two different single-strand homo-oligonucleotides (either dT_{17} or dA_{17}), one labeled with cyanine 3 (Cy3) and the other with the complementary cyanine 5 (Cy5). The use of double-stranded oligonucleotides allowed for the precise control of the distance between the donor and the acceptor. Because this distance has a crucial influence on the energy transfer, keeping this parameter constant was essential for demonstrating the effect of the PhBG on the transfer efficiency. Other design details that are highly relevant to study only the effect of the band gap were the use of low and identical dye concentration (100 nM) to avoid aggregation in solution and to ensure similar distribution of dye molecules in both reference and active crystals. The use of the same material for both crystals ensured similar van der Waals and electrostatic interactions between the DNA−dye constructs and the silica spheres. The only structural difference between reference and sample crystal was the size of the spheres (208 and 272 nm), resulting in the different spectral position of the corresponding PhBG. The dye molecules were infiltrated in both the reference ($\lambda_{PhBG} \approx$ 430 nm) and the active ($\lambda_{PhBG} \approx 600$ nm) photonic crystals by dipping these in the nucleotides solution. The artificial opals, based on silica colloids, had been made by vertical deposition. Figure 12 shows how the PhBG, in the spectral region of the donor emission, caused a decrease of its luminescence and an increase of the spontaneous emission of the acceptor. By inspecting the emission spectra, it is clearly visible that the PhBG enhanced the FRET efficiency. In fact, an increase of the energy-transfer efficiency (E_{ET}) from 37% to 61% was reported.

These results were interpreted in terms of the optical LDOS, or the number of photon modes, in the active PhC and in the reference PhC. When the emission spectrum of an excited state overlaps with the PhBG of the crystal surrounding the excited dye molecule, the probability for a radiative relaxation pathway is lowered due to a decrease in the LDOS (see also section 5). If additional relaxation pathways that are not affected by the presence of a band gap exist, i.e., nonradiative pathways, their probability is enhanced. Energy transfer to an acceptor molecule is such a nonradiative relaxation pathway. This is schematically illustrated in Figure 11b.

Although the rate of energy transfer, k_{ET}, is governed by the available energy modes through the Fermi golden rule, it is the influence of the PhBG on the decay time of the donor that plays a role in the original equation calculated by Förster, where the rate of energy transfer can be given as:

$$k_{ET} = \frac{1}{\tau_d}\left(\frac{R_0}{r}\right)^6 \quad (6)$$

where τ_d is the normal decay time of the donor, r is the distance between the donor−acceptor pair, and R_0 is the Förster distance, a defined parameter for each donor−acceptor pair.[96,135]

This interpretation was corroborated by fluorescence lifetime measurements, showing the increase of the lifetime for the donor alone (without acceptor) in the active crystal (see also section 5) but no such increase for the donor−acceptor pair in the active PhC. This indicated the aperture of a (slightly faster) additional nonradiative relaxation path via energy transfer.[150]

Subsequently, Yang et al. reported similar effects using fluorescein and rhodamine B in a CPhC[151] and by doping a $TbPO_4$ inverse opal with Eu^{3+}.[152] In these experiments the dyes were statistically distributed, without any control on the distance between the donor and the acceptor. They concluded that the energy transfer was obviously enhanced due to the photonic structure by comparing the fluorescence from the photonic structures to that from binary disordered templates.

The use of PhCs was also proposed in a recent publication[153] to tune the energy trapped in photosynthesis, in an attempt to combine biology with nanophotonics. However, it should be emphasized that up to now the most used methods to improve fluorescence properties and the efficiency of resonance energy transfer are based on synthetic protocols, using covalent modifications of molecules to stabilize the excited states and to suppress internal motions that would decrease nonradiative deactivation pathways. Unfortunately, the synthetic approaches are time-consuming and very expensive, while environment modifications could produce similar results in a simple way.

FRET is currently employed in organic light-emitting diodes[154] to harvest the triplet states created in the emitting layer using sensitizers.[155] Enhancement of FRET has already been applied to light-emitting diodes in microcavities,[156] and it has been studied for its use in organic light-emitting diodes (OLEDs) recently.[157] It is important to realize that FRET is mainly a Coulombic interaction between singlet states and that between triplets, Dexter energy transfer, which is an electron-exchange process, becomes more prominent over shorter distance. Triplets play an important role in electroluminescence, where electrons and holes are created independently by charge injection at cathode and anode. For the reported photoluminescence studies,[150,152,157] the interactions between singlets are more relevant, because photoexcitation creates mainly singlet excited states from the singlet ground states of the fluorescent molecules.

7. COLLOIDAL PHOTONIC CRYSTALS AND NONLINEAR OPTICS

The influence of the PhCs on the electromagnetic radiation extends beyond the optical linear regime into the nonlinear domain. Since the preliminary studies on the nature of the anomalous behavior of light in the periodic nanostructures, it has been suggested that the PhCs, or more specifically the PhBG, might have also an influence on the optical processes occurring at higher orders. However, most of the theoretical and experimental work dealing with nonlinear optics (NLO) in periodic nanostructures has been done in two-dimensional (2D) PhCs, namely, waveguides, because 3D PhCs are still difficult to produce.[158] Soljačìc and Joannopoulos[159] provide a good overview of the topic of 2D PhCs, which includes microcavities[160] and nanocavities.[161] The research on the effects of PhCs in the nonlinear optical regime becomes more difficult, resulting in less publications for the case of 3D structures.

7.1. Phase Matching

To our knowledge, the first experimental report was published in 1997 by Martorell et al.[162] In their paper they study the second harmonic generation (SHG) in a low packing opal from 115 nm diameter PS spheres coated with a layer of nonlinearly active molecules. The beads, covered with Malachite Green, were deposited forming a crystal using a cell containing an ion-exchange resin. By this method the separation between the spheres can be tuned, varying the concentration of the colloidal suspension. The sample was excited with a laser emitting at 1064 nm; the incident beam was polarized parallel to the plane of incidence. By using a monochromator, the generated second harmonic (SH) beam, at 532 nm,

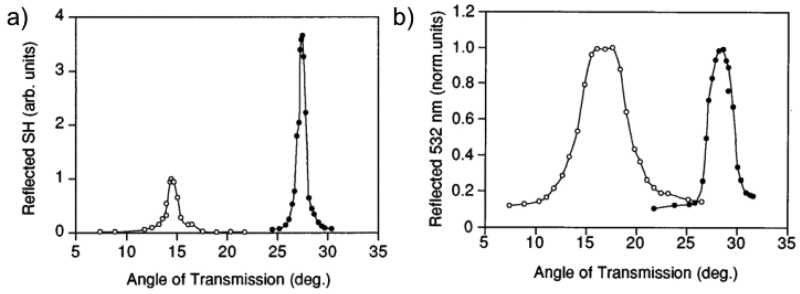

Figure 13. (a) SH intensities and (b) band gaps measured in reflection for two different sphere concentrations in a colloidal suspension containing a nonlinear material.[162] Reprinted with permission from ref 162. Copyright 1997 American Institute of Physics.

was collected in reflection as a function of the angle, giving rise to an increase of intensity of reflected SH at certain angles (see Figure 13). A maximum SH intensity was found to be at the band-gap edge, where the phase lag between the fundamental and the SH beam is overcome due to a decrease in the effective refractive index. The dependence of the SH intensity with the distance between planes, controlled with the concentration of particles in the suspension, and therefore with the position of the band gap, was also demonstrated.

In the case of colloidal PhCs where the building blocks are spheres, the reader might be tempted to postulate that even-order nonlinear optical effects would be negligible because of the centrosymmetric arrangement. Because a spherical distribution of noncentrosymmetric molecules would lead to a centrosymmetric material at the macroscopic level, generation of a second-order response is forbidden in the electric dipole approximation. Indeed, for centrosymmetric materials,[163,164] all microscopic susceptibility tensor components are zero, and as a consequence, second-order nonlinear optical effects are not observed in centrosymmetric crystals. However, a second-order response can be generated from higher-order multipolar contributions by using spheres that are smaller in size than the coherence length of the incident light, as confirmed by theoretical and experimental work.[165−167]

The concept of phase matching is a common point for NLO and PhCs, because phase matching is an important condition for the generation of nonlinear harmonics and because it has also been designated as an inherent property in periodic structures. In the case of second-order NLO, the phase-matching condition arises from the interference between the two incident waves, ω_1 and ω_2, with the generated wave, ω_3, which can lead to destructive interferences or to a coherent effect. It can be mathematically demonstrated[168] that the interference will be constructive when the momentum is conserved

$$\vec{k}_3 = \vec{k}_1 + \vec{k}_2 + \vec{G} \quad (7)$$

where $\vec{k}$ is the wave vector and $\vec{G}$ is the reciprocal lattice vector, which is zero in a uniform material. In this case, the phase-matching problem is normally overcome by using a strongly birefringent crystal that will provide the necessary conditions for the phase matching, based on the different refractive index for ordinary and extraordinary wave.[169]

In the case of PhCs, $\vec{G}$ can be manipulated and the phase matching might be provided naturally by the periodic nanostructure. Indeed, the effect of the phase matching in periodic structures was already reported thoroughly in 1962 by Armstrong et al.,[170] and it has been further exploited in quasi-phase-matching (QPM) structures,[171] a technique that allows almost perfect phase matching between two harmonics by conserving the momentum through an additional momentum contribution corresponding to the wave vector of the periodic structure, in the same way as in nonlinear photonic structures.[172]

Also, the anisotropy of the PhCs with different packing for each plane gives rise to birefringence. By calculating the refractive index for the different directions, one can find the phase-matching direction in the crystal.[173] The results can be later related to the polarization dependence of the second harmonic signal and to the second harmonic intensity, in good agreement with the predictions.

The effect of the phase matching is expected at the PhBG edges[174] and not at the peak where the group velocity (v_g) tends to be zero, as was observed experimentally by Fedyanin et al.[175] In their paper they measure the variation of the SH intensity when the fundamental wavelength is tuned over the spectral range of the PhBG (see Figure 14c). The nanostructure studied is an opal of silica spheres infiltrated with silicon by thermal vapor deposition (see Figure 14a). The size of the spheres, 245 nm diameter, and the refractive index contrast between the silicon and the silica set the PhBG at 870 nm measured under reflection at different angles. The fundamental beam, tunable from 800 to 1000 nm, is linearly polarized and directed to the opal under an angle. The SH beam is filtered and collected with a photomultiplier in reflection. A maximum SH intensity is recorded 20 nm red-shifted from the PhBG peak measured under the same angle. This signal is 50 times higher than that measured outside the PhBG. Furthermore, PhCs are believed to perfectly phase match also counter propagating waves inside the periodic nanostructure.[176]

7.2. Group Velocity

Although the first studies attributed the enhancement of nonlinearities in the PhCs exclusively to birefringence or to phase matching,[177,178] which should be strongly influent in the case of the more exotic nonlinear PhCs,[179,172,180] in recent publications the effect of the group velocity (v_g)[181] has acquired more importance. This effect has been specifically studied in slow-light waveguides.[182,183]

In another experiment performed in 2009 also by the group of Martorell,[181] the effect of the PhBG at the wavelength corresponding to the fundamental beam was studied. Polystyrene spheres (380 nm diameter) coated with Crystal Violet, modified to allow chemical bonding, were deposited, forming a photonic crystal with a band gap centered at 810 nm. The sample was excited using a tunable laser in a range from 720 to 880 nm. In the experiment the laser is tuned while the SH

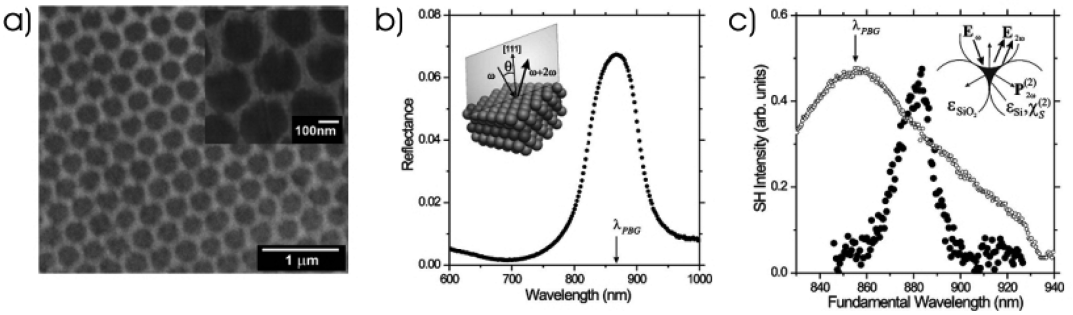

Figure 14. (a) FESEM image of the silicon inverse opal, (b) reflection spectrum of the opal, and (c) spectral dependence of the SH intensity of the wave reflected from the opal.[175] Reprinted with permission from ref 175. Copyright 2005 American Institute of Physics.

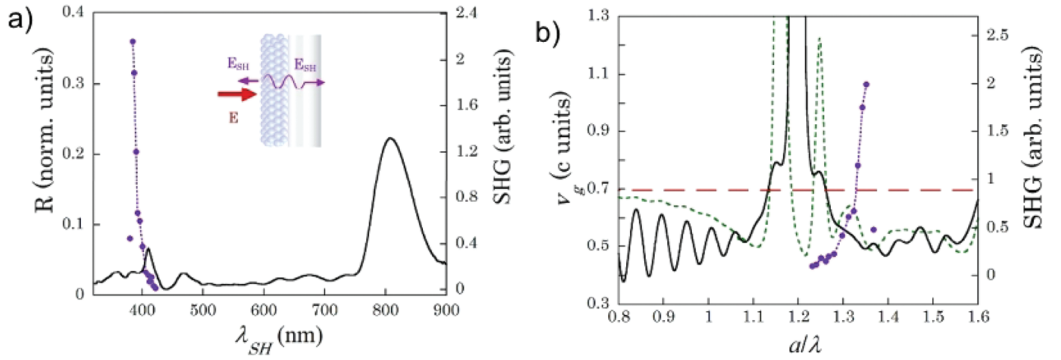

Figure 15. (a) Photonic band gap (black solid curve) with SHG intensity (violet dots) and (b) numerical calculations for reflected (solid line) and transmitted (green dotted line) wave group velocity and SHG intensity (violet dots). The red line is a constant average group velocity for the fcc close-packed structure.[181] Reprinted with permission from ref 181. Copyright 2009 Optical Society of America.

signal is recorded using a monochromator and a photomultiplier tube (see Figure 15a). A ratio of 15 between the SH beam generated at 768 nm and the one generated at 840 nm was found, but no noticeable variation was induced when the crystal plane was varied up to 12°. However, in the same manner as in their former experiment back in 1997, the SH enhancement did not occur exactly at the wavelength of the PhBG but at slightly lower wavelengths. Unlike for the previous interpretation, where the effects of the PhC on the nonlinear optical response were attributed to phase-matching effects, in this case the thickness of the PhC is shorter than the coherence length for phase matching, and that conclusion appears to be no longer valid. They attribute the enhancement of the SH intensity to anomalous group velocities calculated for the flat bands of the photonic band structure (see Figure 15b). In the vicinity of the PhBG the group velocity decreases, which is supported in the paper by theoretical calculations using the multiple-scattering Korringa–Kohn–Rostoker method.[184−186] A slower v_g implies a longer interaction time between light and matter, explaining the more efficient SHG.

It is possible to measure the group velocities in 3D and colloidal PhCs by means of phase measurements, because a phase shift in the propagating beam can be originated in the sample[187] and this shift is related to the delay time caused by partially ordered structures. Scattering and interference can also give rise to localized light modes[188] in an appropriate dielectric microstructure when the scale of the coherent multiple scattering is reduced to the wavelength itself, which is similar to the Anderson localization of electron wave

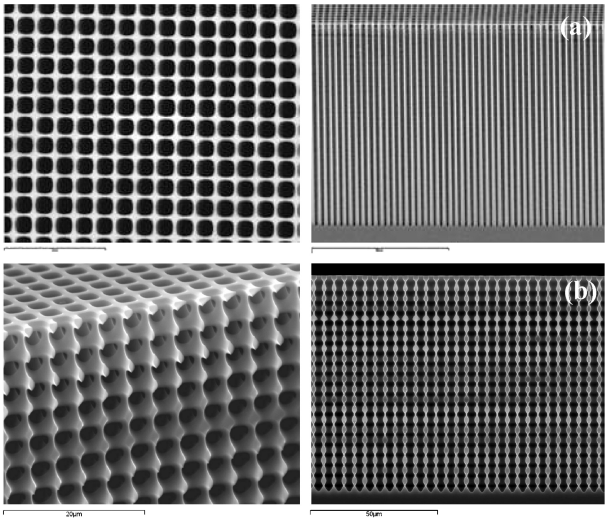

Figure 16. SEM pictures of (a) a 2D and (b) a 3D macroporous silicon template.[191] Reprinted with permission from ref 191. Copyright 2009 Elsevier.

functions in disordered solids. Mathematically, the group velocity is written as

$$v_g = \left(\frac{d\omega}{d\phi}\right) \quad (8)$$

where ϕ is the phase delay and ω is the angular frequency.

The existence of negative group velocities in 3D colloidal PhCs and the possibility to perform a transition from negative to slow-light regime has already been reported[189,190] for short wavelengths, where Bragg diffraction is dominated by non-(111) crystallographic planes and the system displays a truly 3D nature. In the paper from Galisteo-López et al.,[189] a linear relation between the v_g and the number of planes is given. The group velocity is still derived from the phase even in the presence of extinction, and the experimental results are in concordance with the theoretical calculations.

Recently, new procedures for fabricating PhCs out of materials with nonlinear optical properties have been presented by Carvajal et al.,[191] where the nanostructured material was patterned by different etching methods and the nonlinear material was grown in the cast (see Figure 16).

Another exciting subject involves NLO polymers, a discipline that encloses its own difficulties. In general, to make a CPhC one needs first to generate spheres in suspension with a low size polydispersity. Then, a good method to pack these spheres in an ordered fashion is needed, and finally, the structure must be stable when attached to the substrate. Polymers pose challenges to employ because either the colloids are polydisperse, they do not tend to self-assembly, or it is difficult to grow them on a substrate.[192] Still, the great versatility of polymers[193] makes them very interesting for technological applications. Furthermore, many polymers exhibit nonlinear properties or can be doped with nonlinear optical chromophores.[194] Also, by changing the properties of the polymer one can influence the nonlinear response, which allows one to tune the nonlinear optical properties of the material with the pressure, the temperature, or the strain.[195] Therefore, the challenge now is to find a polymer with nonlinear properties that can be synthesized in monodisperse nanospheres that pack in a periodic fashion.

8. CONCLUSIONS

Colloidal photonic crystals can be made up of a large variety of materials, making use of the numerous techniques for their deposition and considering the requirements of the application intended. The efforts made by many research groups in the last two decades have improved the fabrication of CPhCs up to the quality and versatility suitable for the study of their photonic properties. Many of the investigations made in these decades were focused on the emission and light generation inside of the photonic structure because it influences directly the energy levels of the molecule or atom emitting.

The researchers concluded that, using density of states formalism, the study of wave propagation in periodic media is much more simplified than when explained simply by diffraction and reflection of light. The studies suggest that the PhBG is in fact a modification of the density of states with all the consequences involved. For example, the absence of allowed states prohibits the propagation of light with the corresponding wavelength, and as the PhBG is a direct consequence of the periodicity of the material, an interruption of it will create a defect state, which is an induced mode that can be controlled and used to our advantage.

The absence of allowed states extends the lifetime of the excited states when the light is trapped in the material, and because the emission rate is directly related to the modification of the environment, the emission of a dye embedded in a periodic nanostructure can be manipulated. The nonexponential decay times observed in the emission from dyes embedded in a PhC have been theoretically and experimentally linked to the orientation of the density of states and depend strongly on the location of the dye, either in the low or in the high refractive index material. Because of the variation of the density of states along the PhBG, the effect differs greatly at the peak and at the edges of the stop band.

The suppression of the emission by modification of the density of states finds an application in resonance energy transfer, where the efficiency of the optical confinement produced by the photonic crystal has been demonstrated. The lack of available modes increases the transfer of energy from the donor to the acceptor, which can be proven by comparing the decay profiles of the radiative signal in the presence or absence of the PhC and in the presence or absence of the energy-transfer processes.

Finally, the enhancement of SH intensity on a colloidal PhC was demonstrated in several experiments and confirmed by theoretical simulations. Nevertheless, the relevance of the different phenomena occurring in the PhC in terms of nonlinear optical response is not completely resolved. Both the phase matching, essential in nonlinear processes, and the group velocity, which would explain increases of the second harmonic signal, might have an influence on the results. Although there are still many open questions, it is clear that NLO effects can benefit from PhCs for intensity enhancement, as well as for guiding the second-order light wave.

AUTHOR INFORMATION

Corresponding Author

*E-mail: Branko.Kolaric@umons.ac.be; Koen.Clays@fys.kuleuven.be.

BIOGRAPHIES

Kasper Baert received his Master in Chemistry in 2005 and his Ph.D. in Chemistry in 2010 from the Catholic University of Leuven. His research interests lie in the field of colloidal photonic crystals, more particularly in fluorescence phenomena occurring in these structures and the effects of these on nonlinear optical properties. He is currently active as R&D engineer at Photovoltech, involved in the development of solar cells.

Luis González-Urbina received his Master in Physical Chemistry in 2005 from the University of the Basque Country and the Master in Material Engineering for microelectronics from the Catholic University of Leuven in 2006, where he is currently a Ph.D. candidate in Chemistry. His research is focused on colloidal photonic crystals: synthesis, deposition techniques, emission, and energy transfer.

Branko Kolaric obtained his Ph.D. from TU-Berlin (Berlin, Germany) in the field of physics and physical chemistry of polyelectrolytes. After his Ph.D. he has worked as a researcher for leading European research institutions such as Max Planck Institute for Molecular Physiology, University of Osnabruck, and the Catholic University of Leuven. In 2011, he became Full Research Professor, awarded by the Ministry of Science of the Republic of Serbia. At the moment, he is a senior researcher at INFLUX lab, University of Mons. His research interests cover various aspects of photonics and plasmonics.

Koen Clays obtained his Ph.D. in Chemistry in 1989 at the Catholic University of Leuven. After a postdoc at Eastman-Kodak (Rochester, New York), he obtained a professor position at the Department of Chemistry, Catholic University of Leuven, Belgium. He is also an adjunct professor at the Department of Physics and Astronomy, Washington State University, Pullman, Washington. His research interests are linear and nonlinear optics of molecular and nanostructured materials, including research on photonic crystals and complex organic materials for second-order nonlinear optics.

Dr. Javier Perez-Moreno holds two undergraduate degrees in Physics from University of Valencia (Spain) and University of Leeds (UK) and a M.S. in Physics from Washington State University (USA). In 2007 he obtained a Ph.D. in Physics (from Washington State University) and a Ph.D. in Chemistry (from the K.U.Leuven, Belgium) from his work on the optimization of the molecular nonlinear optical response. Currently, he is a postdoctoral research at the K.U.Leuven, where he focuses on the study, characterization, and optimization of the organic molecular response using the Thomas−Kuhn sum rules.

ACKNOWLEDGMENT

B.K. warmly acknowledges financial support from F.N.R.S. and from Smart film grant 830039 (ECV12020020892F) in the framework of Convergence project. J.P-M. acknowledges the K.U.Leuven IDO project 3E090505. The authors would like to thank Dr. RAL Vallée and Dr. W. Libaers for the discussions on this work and J. Graham for copyediting and language assistance.

REFERENCES

(1) Lifante, G.; Wiley, J. *Integrated photonics: Fundamentals*; Wiley Online Library: New York, 2003.
(2) Parker, G.; Charlton, M. *Phys. World* **2000**, *13*, 29.
(3) Chutinan, A.; Noda, S. *Appl. Phys. Lett.* **1999**, *75*, 3739.
(4) Park, H.-G.; Kim, S.-H.; Kwon, S.-H.; Ju, Y.-G.; Yang, J.-K.; Baek, J.-H.; Kim, S.-B.; Lee, Y.-H. *Science* **2004**, *305*, 1444.
(5) Noda, S. *Science* **2006**, *314*, 260.
(6) Coldren, L. A.; Corzine, S. W.; Coldren, L. A. *Diode lasers and photonic integrated circuits*; Wiley: New York, 1995.
(7) Kosaka, H.; Kawashima, T.; Tomita, A.; Notomi, M.; Tamamura, T.; Sato, T.; Kawakami, S. *Phys. Rev. B: Condens. Matter* **1998**, *58*, 10096.
(8) Busch, K. *Photonic crystals: Advances in design, fabrication and characterization*; Wiley-VCH: New York, 2004.
(9) Zhang, W.; Zhang, D.; Fan, T.; Gu, J.; Ding, J.; Wang, H.; Guo, Q.; Ogawa, H. *Chem. Mater.* **2009**, *21*, 33.

(10) Cai, W.; Vladimir, S. *Optical metamaterials. Fundamental Applications*; Springer: New York, 2009.
(11) Henzie, J.; Lee, J.; Lee, M. H.; Hasan, W.; Odom, T. W. *Annu. Rev. Phys. Chem.* **2009**, *60*, 147.
(12) Ozbay, E. *Science* **2006**, *311*, 189.
(13) Joannopoulos, J. D.; Johnson, S. G.; Winn, J. N.; Meade, R. D. *Photonic Crystals: Molding the Flow of Light*, 2nd ed.; Princeton University Press: Princeton, NJ, 2008.
(14) Moon, J. H.; Yang, S. *Chem. Rev.* **2010**, *110*, 547.
(15) Takiguchi, Y. *J. Phys. Conf. Ser.* **2008**, *109*, 012004.
(16) Cosgrove, T. *Colloid Science: Principles, methods and applications*; Wiley: Bristol, U.K., 2005.
(17) Stöber, W.; Fink, A.; Bohn, E. *J. Colloid Interface Sci.* **1968**, *26*, 62.
(18) Mahshid, S.; Askari, M.; Ghamsari, M. *J. Mater. Process. Technol.* **2007**, *189*, 296.
(19) Andreescu, D.; Matijevic, E.; Goia, D. *Colloids Surf., A* **2006**, *291*, 93.
(20) Poehlein, G., Ottewill, R. H., Goodwin, J. W., Eds. *Science and technology of polymer colloids, Vol. II*; Martinus Nijhoff Publishers: Boston, 1983.
(21) Arshady, R. *Colloid Polym. Sci.* **1992**, *270*, 717.
(22) Reese, C. E.; Guerrero, C. D.; Weissman, J. M.; Lee, K.; Asher, S. A. *J. Colloid Interface Sci.* **2000**, *232*, 76.
(23) Tse, A. S.; Wu, Z.; Asher, S. A. *Macromolecules* **1995**, *28*, 6533.
(24) Perro, A.; Reculusa, S.; Ravaine, S.; Bourgeat-Lami, E.; Duguet, E. *J. Mater. Chem.* **2005**, *15*, 3745.
(25) Ding, T.; Liu, Z.-F.; Song, K.; Clays, K.; Tung, C.-H. *Langmuir* **2009**, *25*, 10218.
(26) Ding, T.; Song, K.; Clays, K.; Tung, C.-H. *Adv. Mater.* **2009**, *21*, 1936.
(27) Galisteo-López, J. F.; Ibisate, M.; Sapienza, R.; Froufe-Pérez, L. S.; Blanco, A.; López, C. *Adv. Mater.* **2010**, *XX*, 1.
(28) Kim, S.-H.; Lee, S. Y.; Yang, S.-M.; Yi, G.-R. *NPG Asia Mater.* **2011**, *3*, 23.
(29) Jiang, P.; Bertone, J. F.; Hwang, V. L., K. S.; Colvin *Chem. Mater.* **1999**, *11*, 2132.
(30) Wong, S.; Kitaev, V.; Ozin, G. A. *J. Am. Chem. Soc.* **2003**, *125*, 15589.
(31) Kuai, S. L.; Hu, X. F.; Hache, A.; Truong, V. V. *J. Cryst. Growth* **2004**, *267*, 317.
(32) Míguez, H.; Meseguer, F.; López, C.; Blanco, A.; Moya, J. S.; Requena, J.; Mifsud, A.; Fornés, V. *Adv. Mater.* **1998**, *10*, 480.
(33) Yan, Q.; Zhao, X. S.; Zhou, Z. *J. Cryst. Growth* **2006**, *288*, 205.
(34) Peschel, S.; Schmid, G. *Angew. Chem., Int. Ed.* **1995**, *34*, 1442.
(35) Bevan, M. A.; Lewis, J. A.; Braun, P. V.; Wiltzius, P. *Langmuir* **2004**, *20*, 7045.
(36) Jiang, P. *Langmuir* **2006**, *22*, 3955.
(37) Kim, E.; Xia, Y.; Whitesides, G. M. *Adv. Mater.* **1996**, *8*, 245.
(38) Park, S. H.; Xia, Y. *Langmuir* **1999**, *15*, 266.
(39) Kenis, P. J. A.; Ismagilov, R. F.; Whitesides, G. M. *Science* **1999**, *285*, 83.
(40) Yi, G. R.; Moon, J. H.; Yang, S. M. *Adv. Mater.* **2001**, *15*, 1185.
(41) Jiang, P.; McFarland, M. J. *J. Am. Chem. Soc.* **2004**, *126*, 13778.
(42) Mihi, A.; Ocaña, M.; Míguez, H. *Adv. Mater.* **2006**, *18*, 2244.
(43) Bardosova, M.; Pemble, M. E.; Povey, I. M.; Tredgold, R. H. *Adv. Mater.* **2010**, *22*, 3104.
(44) Wang, H.; Yan, K. P.; Xie, J.; Duan, M. *Mater. Sci. Semicond. Process.* **2008**, *11*, 44.
(45) Jiang, P.; Prasad, T.; McFarland, M. J.; Colvin, V. L. *Appl. Phys. Lett.* **2006**, *89*, 011908.
(46) van Blaaderen, A.; Ruel, R.; Wiltzius, P. *Nature* **1997**, *385*, 321.
(47) Woodcock, L. V. *Nature* **1997**, *385*, 141.
(48) Bruce, A. D.; Wilding, N. B.; Ackland, G. J. *Phys. Rev. Lett.* **1997**, *79*, 3002.
(49) Pusey, P. N.; Vanmegen, W.; Bartlett, P.; Ackerson, B. J.; Rarity, J. G.; Underwood, S. M. *Phys. Rev. Lett.* **1989**, *63*, 2753.
(50) Woodcock, L. V. *Nature* **1997**, *388*, 236.
(51) Norris, D. J.; Arlinghaus, E. G.; Meng, L. L.; Heiny, R.; Scriven, L. E. *Adv. Mater.* **2004**, *16*, 1393.
(52) Sze, S. M. *Physics of Semiconductor Devices*, 3rd ed.; Wiley Interscience: New York, 2006.
(53) Born, M.; Wolf, E. *Principles of Optics: Electromagnetic Theory of Propagation, Interference and Diffraction of Light*, 7th ed.; Cambridge University Press: Cambridge, U.K., 1999.
(54) Brooker, G. *Modern Classical Optics*, 1st ed.; Oxford University Press: Oxford, U.K., 2003.
(55) Aspnes, D. E. *Thin Solid Films* **1982**, *89*, 249.
(56) Fujikawa, R.; Baryshev, A.; Nishimura, K.; Uchida, H.; Inoue, M. *J. Porous Mater.* **2006**, *13*, 287.
(57) Heavens, O. *Optical properties of thin solid films*; Courier Dover Publications: New York, 1991.
(58) Kettle, S. F. A.; Norrby, L. J. *J. Chem. Educ.* **1990**, *67*, 1022.
(59) Griffiths, D. J. *Introduction to Quantum Mechanics*; Benjamin-Cummings Pub. Co.: New Jersey, 2004.
(60) King, J. S.; Graugnard, E.; Summers, C. J. *Adv. Mater.* **2005**, *17*, 1010.
(61) Marichy, C.; Dechézelles, J. F.; Willinger, M. G.; Pinna, N.; Ravaine, S.; Vallée, R. A. L. *Nanoscale* **2010**, *2*, 786.
(62) Oskooi, A. F.; Roundy, D.; Ibanescu, M.; Bermel, P.; Joannopoulos, J. D.; Johnson, S. G. *ChemPhysChem* **2010**, *181*, 687.
(63) Taflove, A.; Hagness, S. C. *Computational Electrodynamics: The Finite-Difference Time-Domain Method*, 3rd ed.; Artech House: Boston, 2005.
(64) Yee, K. *IEEE Trans. Antennas Propagation* **1966**, *14*, 302.
(65) Matsushita, S.; Suavet, O.; Hashiba, H. *Electrochim. Acta* **2010**, *55*, 2398.
(66) Kaneko, K.; Sun, H. B.; Duan, X. M.; Kawata, S. *Appl. Phys. Lett.* **2003**, *83*, 2091.
(67) García-Santamaría, F.; López, C.; Meseguer, F.; López-Tejeira, F.; Sánchez-Dehesa, J.; Miyazaki, H. T. *Appl. Phys. Lett.* **2001**, *79*, 2309.
(68) Noda, S.; Tomoda, K.; Yamamoto, N.; Chutinan, A. *Science* **2000**, *289*, 604.
(69) Ren, Z.; Zhai, T.; Wang, Z.; Zhou, J.; Liu, D. *Adv. Mater.* **2008**, *20*, 2337.
(70) Kolaric, B.; Vandeparre, H.; Fabian, B.; Damman, P. *submitted for publication*.
(71) Schroden, R. C.; Al-Daous, M.; Blanford, C. F.; Stein, A. *Chem. Mater.* **2002**, *14*, 3305.
(72) Liu, Z.-F.; Ding, T.; Zhang, G.; Song, K.; Clays, K.; Tung, C.-H. *Langmuir* **2008**, *24*, 10519.
(73) Blanco, A.; Chomski, E.; Grabtchak, S.; Ibisate, M.; John, S.; Leonard, S. W.; López, C.; Meseguer, F.; Míguez, H.; Mondia, J. P.; Ozin, G. A.; Toader, O.; van Driel, H. M. *Nature* **2000**, *405*, 437.
(74) Kelly, A.; Groves, G. W.; Kidd, P. *Crystallography and crystal defects*; John Wiley & Sons Inc: New York, 2000.
(75) Vanacken, J.; Vinckx, W.; Moshchalkov, V. V.; Mátéfi-Tempfli, S.; Mátéfi-Tempfli, M.; Michotte, S.; Piraux, L.; Ye, X. *Phys. C* **2008**, *468*, 585.
(76) Macleon, H. A. *Thin-Film Optical Filters*, 3rd ed.; Institute of Physics Publishing: Bristol, U.K., 2001.
(77) Baert, K.; Kolaric, B.; Libaers, W.; Vallée, R. A. L.; Di Vece, M.; Lievens, P.; Clays, K. *Res. Lett. Nanotechnol.* **2008**, *2008*, 974072.
(78) Noda, S.; Chutinan, A.; Imada, M. *Nature* **2000**, *407*, 608.
(79) Yan, Q.; Chen, A.; Chua, S. J.; Zhao, X. S. *Adv. Mater.* **2005**, *17*, 2849.
(80) Jun, Y.; Leatherdale, C. A.; Norris, D. J. *Adv. Mater.* **2005**, *17*, 1908.
(81) Wostyn, K.; Zhao, Y.; de Schaetzen, G.; Hellemans, L.; Matsuda, N.; Clays, K.; Persoons, A. *Langmuir* **2003**, *19*, 4465.
(82) Zhao, Y.; Wostyn, K.; de Schaetzen, G.; Clays, K.; Hellemans, L.; Persoons, A.; Szekeres, M.; Schoonheydt, R. A. *Appl. Phys. Lett.* **2003**, *82*, 3764.
(83) Tétreault, N.; Mihi, A.; Míguez, H.; Rodríguez, I.; Ozin, G. A.; Meseguer, F.; Kitaev, V. *Adv. Mater.* **2004**, *16*, 346.
(84) Colodrero, S.; Ocaña, M.; Míguez, H. *Langmuir* **2008**, *24*, 4430.

(85) Pozas, R.; Mihi, A.; Ocaña, M.; Míguez, H. *Adv. Mater.* **2006**, *18*, 1183.
(86) Colodrero, S.; Ocaña, M.; González-Elipe, R.; Míguez, H. *Langmuir* **2008**, *24*, 9135.
(87) Massé, P.; Reculusa, S.; Clays, K.; Ravaine, S. *Chem. Phys. Lett.* **2006**, *422*, 251.
(88) Massé, P.; Pouclet, G.; Ravaine, S. *Adv. Mater.* **2008**, *20*, 584.
(89) Massé, P.; Ravaine, S. *Colloids Surf., A* **2005**, *270*, 148.
(90) Reculusa, S.; Massé, P.; Ravaine, S. *J. Colloid Interface Sci.* **2004**, *279*, 471.
(91) Dechézelles, J.-F.; Massé, P.; Cloutet, E.; Cramail, H.; Ravaine, S. *Colloids Surf., A* **2009**, *343*, 8; 22nd Conference of the European-Colloid-and-Interface-Society, Cracow, Poland, Aug 31−Sep 05, 2008.
(92) Massé, P.; Vallée, R. A. L.; Dechézelles, J. F.; Rosselgong, J.; Cloutet, E.; Cramail, H.; Zhao, X. S.; Ravaine, S. *J. Phys. Chem. C* **2009**, *113*, 14487.
(93) Yan, Q.; Zhou, Z.; Zhao, X. S. *Langmuir* **2005**, *21*, 3158.
(94) Baert, K.; Song, K.; Vallée, R. A. L.; Van der Auweraer, M.; Clays, K. *J. Appl. Phys.* **2006**, *100*, 123112.
(95) Stokes, G. G. *Philos. Trans. R. Soc. London* **1852**, *142*, 463.
(96) Lakowicz, J. R. *Principles of Fluorescence Spectroscopy*, 2nd ed.; Kluwer Academic/Plenum Publishers: Amsterdam, The Netherlands, 1999.
(97) Yablonovitch, E. *Phys. Rev. Lett.* **1987**, *58*, 2059.
(98) John, S.; Wang, J. *Phys. Rev. Lett.* **1990**, *64*, 2418.
(99) John, S.; Wang, J. *Phys. Rev. B: Condens. Matter* **1991**, *43*, 12772.
(100) Tomljenovic-Hanic, S.; Ankiewicz, A. *Opt. Commun.* **2004**, *237*, 351.
(101) Bogomolov, V. N.; Gaponenko, S. V.; Germanenko, I. N.; Kapitonov, A. M.; Petrov, E. P.; Gaponenko, N. V.; Prokofiev, A. V.; Ponyavina, A. N.; Silvanovich, N. I.; Samoilovich, S. M. *Phys. Rev. E: Stat. Phys. Plasmas Fluids Relat. Interdiscip. Top.* **1997**, *55*, 7619.
(102) Yamasaki, T.; Tsutsui, T. *Appl. Phys. Lett.* **1998**, *72*, 1957.
(103) Blanco, A.; López, C.; Mayoral, R.; Míguez, H.; Meseguer, F.; Mifsud, A.; Herrero, J. *Appl. Phys. Lett.* **1998**, *73*, 1781.
(104) Megens, M.; Wijnhoven, J. E. G. J.; Lagendijk, A.; Vos, W. L. *J. Opt. Soc. Am. B* **1999**, *16*, 1403.
(105) Song, K.; Vallée, R. A. L.; Van der Auweraer, M.; Clays, K. *Chem. Phys. Lett.* **2006**, *421*, 1.
(106) Martorell, J.; Lawandy, N. M. *Phys. Rev. Lett.* **1990**, *65*, 1877.
(107) Tong, B. Y.; John, P. K.; Zhu, Y.-T.; Liu, Y. S.; Wong, S. K.; Ware, W. R. *J. Opt. Soc. Am. B* **1993**, *10*, 356.
(108) Petrov, E. P.; Bogomolov, V. N.; Kalosha, I. I.; Gaponenko, S. V. *Phys. Rev. Lett.* **1998**, *81*, 77.
(109) Megens, M.; Schriemer, H. P.; Lagendijk, A.; Vos, W. L. *Phys. Rev. Lett.* **1999**, *83*, 5401.
(110) Petrov, E. P.; Bogomolov, V. N.; Kalosha, I. I.; Gaponenko, S. V. *Phys. Rev. Lett.* **1999**, *83*, 5402.
(111) Megens, M.; Wijnhoven, J. E. G. J.; Lagendijk, A.; Vos, W. L. *Phys. Rev. A: At., Mol., Opt. Phys.* **1999**, *59*, 4727.
(112) Loudon, R. *The Quantum Theory of Light*; Clarendon Press: Oxford, U.K., 1973.
(113) Schriemer, H. P.; van Driel, H. M.; Koenderink, A. F.; Vos, W. L. *Phys. Rev. A: At., Mol., Opt. Phys.* **2000**, *63*, 011801.
(114) Koenderink, A. F.; Bechger, L.; Schrieme, H. P.; Lagendijk, A.; Vos, W. L. *Phys. Rev. Lett.* **2002**, *88*, 143903.
(115) Koenderink, A. F.; Bechger, L.; Lagendijk, A.; Vos, W. L. *Phys. Status Solidi A* **2003**, *197*, 648.
(116) Nikolaev, I. S.; Lodahl, P.; van Driel, A. F.; Koenderink, A. F.; Vos, W. L. *Phys. Rev. B: Condens. Matter Mater. Phys.* **2007**, *75*, 115302.
(117) Vallée, R. A. L.; Baert, K.; Kolaric, B.; Van der Auweraer, M.; Clays, K. *Phys. Rev. B: Condens. Matter Mater. Phys.* **2007**, *76*, 045113.
(118) Lodahl, P.; Floris van Driel, A.; Nikolaev, I. S.; Irman, A.; Overgaag, K.; Vanmaekelbergh, D.; Vos, W. L. *Nature* **2004**, *430*, 654.
(119) Bechger, L.; Lodahl, P.; Vos, W. L. *J. Phys. Chem. B* **2005**, *109*, 9980.
(120) Nikolaev, I. S.; Lodahl, P.; Vos, W. L. *Phys. Rev. A: At., Mol., Opt. Phys.* **2005**, *71*, 053813.
(121) Barth, M.; Gruber, A.; Cichos, F. *Phys. Rev. B: Condens. Matter Mater. Phys.* **2005**, *72*, 085129.
(122) Li, M.; Zhang, P.; Li, J.; Zhou, J.; Sinitskii, A.; Abramova, V.; Klimonsky, S. O.; Tretyakov, Y. D. *Appl. Phys. B: Lasers Opt.* **2007**, *89*, 251.
(123) Aloshyna, M.; Sivakumar, S.; Venkataramanan, M.; Brolo, A. G.; van Veggel, F. C. J. M. *J. Phys. Chem. C* **2007**, *111*, 4047.
(124) Barth, M.; Schuster, R.; Gruber, A.; Cichos, F. *Phys. Rev. Lett.* **2006**, *96*, 243902.
(125) Sprik, R.; van Tiggelen, B. A.; Lagendijk, A. *Europhys. Lett.* **1996**, *35*, 265.
(126) Brzezinski, A.; Lee, J.-T.; Slinker, J. D.; Malliaras, G. G.; Braun, P. V.; Wiltzius, P. *Phys. Rev. B: Condens. Matter Mater. Phys.* **2008**, *77*, 233106.
(127) Vion, C.; Barthou, C.; Bénalloul, P.; Schwob, C.; Coolen, L.; Gruzintev, A.; Emelchenko, G.; Masalov, V.; Frigerio, J.-M.; Maître, A. *J. Appl. Phys.* **2009**, *105*, 113120.
(128) Yoshino, K.; Lee, S. B.; Tatsuhara, S.; Kawagishi, Y.; Ozaki, M.; Zakhidov, A. A. *Appl. Phys. Lett.* **1998**, *73*, 3506.
(129) Yoshino, K.; Tatsuhara, S.; Kawagishi, Y.; Ozaki, M.; Zakhidov, A. A.; Vardeny, Z. V. *Appl. Phys. Lett.* **1999**, *74*, 2590.
(130) Gaponik, N.; Eychmüller, A.; Rogach, A. L.; Solovyev, V. G.; Torres, C. M. S.; Romanov, S. G. *J. Appl. Phys.* **2004**, *95*, 1029.
(131) Gérard, J. M.; Sermage, B.; Gayral, B.; Legrand, B.; Costard, E.; Thierry-Mieg, V. *Phys. Rev. Lett.* **1998**, *81*, 1110.
(132) Kaplan, S. F.; Kartenko, N. F.; Kurdyukov, D. A.; Medvedev, A. V.; Golubev, V. G. *Appl. Phys. Lett.* **2005**, *86*, 071108.
(133) King, J. S.; Graugnard, E.; Summers, C. J. *Appl. Phys. Lett.* **2006**, *88*, 081109.
(134) Paquet, C.; Yoshino, F.; Levina, L.; Gourevich, I.; Sargent, E. H.; Kumacheva, E. *Adv. Funct. Mater.* **2006**, *16*, 18926.
(135) Turro, N. J. In *Modern Molecular Photochemistry*; Turro, N. J., Ed.; The Benjamin/Cummings Publishing Co., Inc.: Menlo Park, CA, 1978.
(136) Berney, C.; Danuser, G. *Biophys. J.* **2003**, *84*, 3992.
(137) Oppenheimer, J. R. *Phys. Rev.* **1941**, *60*, 158.
(138) Clegg, R. M. *Biophotonics Int.* **2004**, *11*, 42.
(139) Förster, T. *Ann. Phys.* **1948**, *437*, 55.
(140) Kuriziki, G.; Genack, A. Z. *Phys. Rev. Lett.* **1988**, *61*, 2269.
(141) Kobayashi, T.; Zheng, Q. B.; Sekiguchi, T. *Phys. Rev. A: At., Mol., Opt. Phys.* **1995**, *52*, 2835.
(142) Folan, L. M.; Arnold, S.; Druger, S. D. *Chem. Phys. Lett.* **1985**, *118*, 322.
(143) Andrews, D. L. *Chem. Phys.* **1989**, *135*, 195.
(144) Gersten, J. I.; Nitzan, A. *Chem. Phys. Lett.* **1984**, *104*, 31.
(145) Pineda, A. C.; Ronis, D. *Phys. Rev. E: Stat. Phys. Plasmas Fluids Relat. Interdiscip. Top.* **1995**, *52*, 5178.
(146) Andrew, P.; Barnes, W. L. *Science* **2000**, *290*, 785.
(147) Finlayson, C. E.; Ginger, D. S.; Greenham, N. C. *Chem. Phys. Lett.* **2001**, *338*, 83.
(148) Fujiwara, H.; Sasaki, K.; Masuhara, H. *ChemPhysChem* **2005**, *6*, 2410.
(149) Shibata, K.; Kimura, H.; Tsuchida, A.; Okubo, T. *Colloid Polym. Sci.* **2006**, *285*, 127.
(150) Kolaric, B.; Baert, K.; Van der Auweraer, M.; Vallée, R. A. L.; Clays, K. *Chem. Mater.* **2007**, *19*, 5547.
(151) Yang, Z.; Zhou, X.; Huang, X.; Zhou, J.; Yang, G.; Xie, Q.; Sun, L.; Li, B. *Opt. Lett.* **2008**, *33*, 1963.
(152) Yang, Z.; Huang, X.; Sun, L.; Zhou, J.; Yang, G.; Li, B.; Yu, C. *J. Appl. Phys.* **2009**, *105*, 083523.
(153) Blum, C.; Mosk, A. P.; Nikolaev, I. S.; Subramaniam, V.; Vos, W. L. *Small* **2008**, *4*, 492.
(154) Baldo, M. A.; Lamansky, S.; Burrows, P. E.; Thompson, M. E.; Forrest, S. R. *Appl. Phys. Lett.* **1999**, *75*, 4.
(155) Holder, E.; Langeveld, B. M. W.; Schubert, U. S. *Adv. Mater.* **2005**, *17*, 1109.
(156) Dodabalapur, A.; Rothberg, L.; Jordan, R.; Miller, T.; Slusher, R. *J. Appl. Phys.* **1996**, *80*, 6954.
(157) González-Urbina, L.; Pérez-Moreno, J.; Kolaric, B.; Clays, K. *J. Photonics Energy*, accepted for publication.

(158) Farsari, M.; Ovsianikov, A.; Vamvakaki, M.; Sakellari, I.; Gray, D.; N., C. B.; Fotakis, C. *Appl. Phys. A: Mater. Sci. Process.* **2008**, *93*, 11.
(159) Soljačć, M.; Joannopoulos, J. D. *Nat. Mater.* **2004**, *3*, 211.
(160) Akahane, Y.; Asano, T.; Song, B.; Noda, S. *Nature* **2003**, *425*, 944.
(161) Bravo Abad, J.; Rodríguez, A.; Bermel, P.; Johnson, S. G.; Joannopoulos, J. D.; Soljačć, M. *Opt. Express* **2007**, *24*, 16161.
(162) Martorell, J.; Vilaseca, R.; Corbalán, R. *Appl. Phys. Lett.* **1997**, *70*, 702.
(163) Verbiest, T.; Clays, K.; Rodríguez, V. *Second-Order Nonlinear Optical Characterizations Techniques*; CRC Press: Boca Raton, FL, 2009; p 11.
(164) Reeve, J. E.; Anderson, H. L.; Clays, K. *Phys. Chem. Chem. Phys.* **2010**, *12*, 13484.
(165) Dadap, J. I.; Shan, J.; Eisenthal, K. B.; Heinz, T. F. *Phys. Rev. Lett.* **1999**, *83*, 4045.
(166) Baert, K.; Wostyn, K.; Vallée, R. A. L.; Clays, K. *J. Nonlinear Opt. Phys. Mater.* **2007**, *16*, 27.
(167) Wang, H.; Yan, E. C. Y.; Borguet, E.; Eisenthal, K. B. *Chem. Phys. Lett.* **1996**, *259*, 15.
(168) Sakoda, K. *Optical properties of photonic crystals*; Springer: Berlin, 2004; p 10.
(169) Prasad, P. N.; Williams, D. J. *Introduction to Nonlinear Optical Effects in Molecules and Polymers*; Wiley Interscience: New York, 1991.
(170) Armstrong, J. A.; Bloembergen, N.; Ducuing, J.; Pershan, P. S. *Phys. Rev.* **1962**, *127*, 1918.
(171) Saltiel, S. M.; Sheng, Y.; Voloch-Bloch, N.; Neshev, D. N.; Krolikowski, W.; Arie, A.; Koynov, K.; Kivshar, Y. S. *IEEE J. Quantum Electron.* **2009**, *45*, 1465.
(172) Berger, V. *Phys. Rev. Lett.* **1998**, *81*, 4136.
(173) Golovan, L. A.; Timoshenko, V. Y.; Fedotov, A. B.; Kuznetsova, L. P.; Sidorov-Biryukov, D. A.; Kashkarov, P. K.; Zheltikov, A. M.; Kovalev, D.; Künzner, N.; Gross, E.; Diener, J.; Polisski, G.; Koch, F. *Appl. Phys. B: Laser Opt.* **2001**, *73*, 31.
(174) Sakoda, K.; Ohtaka, K. *Phys. Rev. B: Condens. Matter Mater. Phys.* **1996**, *54*, 5742.
(175) Fedyanin, A. A.; Aktsipetrov, O. A.; Kurdyukov, D. A.; Golubev, V. G.; Inoue, M. *Appl. Phys. Lett.* **2005**, *87*, 151111.
(176) Maymó, M.; Molinos-Gómez, A.; Vidal, X.; Botey, M.; Di Finizio, S.; Domínguez-Juarez, J.; López-Calahorra, F.; Martorell, J. Second order nonlinear processes in photonic crystals, 2005; 7th International Conference on Transparent Optical Networks, Barcelona, Spain, Jul 3−7, 2005.
(177) Lawandy, N. M.; Johnston, S. A.; Martorell, J. *Opt. Commun.* **1988**, *65*, 425.
(178) Bloembergen, N.; Sievers, A. *Appl. Phys. Lett.* **1970**, *17*, 483.
(179) Saltiel, S.; Kivshar, Y. S. *Opt. Lett.* **2000**, *25*, 1204.
(180) Mingaleev, S.; Kivshar, Y. *Opt. Photonics News* **2002**, *13*, 48.
(181) Botey, M.; Maymó, M.; Molinos-Gómez, A.; Dorado, L.; Depine, R. A.; Lozano, G.; Mihi, A.; Míguez, H.; Martorell, J. *Opt. Express* **2009**, *17*, 12210.
(182) Soljačć, M.; Johnson, S. G.; Fan, S.; Ibanescu, M.; Ippen, E.; Joannopoulos, J. D. *J. Opt. Soc. Am. B* **2002**, *19*, 2052.
(183) Villeneuve, A.; Yang, C. C.; Stegeman, G. I.; Lin, C.; Lin, H. *Appl. Phys. Lett.* **1993**, *62*, 2465.
(184) Mavropoulos, P.; Papanikolaou, N. *Comput. Nanosci.: Do It Yourself!* **2006**, *31*, 131.
(185) Korringa, J. *Physica* **1947**, *13*, 392.
(186) Kohn, W.; Rostoker, N. *Phys. Rev.* **1954**, *94*, 1111.
(187) Clays, K.; Wostyn, K.; Zhao, Y.; Persoon, A. *J. Nonlinear Opt. Phys. Mater.* **2002**, *11*, 261.
(188) John, S. *Phys. Today* **1991**, *44*, 32.
(189) Galisteo-López, J. F.; Galli, M.; Balestreri, A.; Patrini, M.; Andreani, L. C.; López, C. *Opt. Express* **2007**, *15*, 15342.
(190) Hai-Ying, L.; Zi-Ming, M.; Qiao-Feng, D.; Li-Jun, W.; Sheng, L.; Song-Hao, L. *Acta Phys. Sin.* **2009**, *58*, 4702.
(191) Carvajal, J. J.; Peña, A.; Kumar, R.; Pujol, M. C.; Mateos, X.; Aguiló, M.; Díaz, F.; Vázquez de Aldana, J. R.; Méndez, C.; Moreno, P.; Roso, L.; Trifonov, T.; Rodríguez, A.; Alcubilla, R.; Král, Z.; Ferré-Borrull, J.; Pallarès, J.; Marsal, L. F.; Di Finizio, S.; Macovez, R.; Martorell, J. *J. Lumin.* **2009**, *129*, 1441.
(192) Zhang, J.; Sun, Z.; Yang, B. *Curr. Opin. Colloid Interface Sci.* **2009**, *14*, 103.
(193) Paquet, C.; Kumacheva, E. *Mater. Today* **2008**, *11*, 48.
(194) Ghebremichael, F.; Kuzyk, M. G.; Lackritz, H. S. *Prog. Polym. Sci.* **1997**, *22*, 1147.
(195) Kerherve, F. *Opt. Commun.* **1973**, *9*, 420.